Syst. Biol. 62(6):878–900, 2013

DOI:10.1093/sysbio/syt053
Advance Access publication August 6, 2013

Bite of the Cats: Relationships between Functional Integration and Mechanical Performance as Revealed by Mandible Geometry

PAOLO PIRAS[1,2,*], LEONARDO MAIORINO[1,2], LUCIANO TERESI[3,4], CARLO MELORO[5], FEDERICO LUCCI[2], TASSOS KOTSAKIS[1,2], AND PASQUALE RAIA[5]

[1]*Center for Evolutionary Ecology, Largo San Leonardo Murialdo 1, 00146, Rome, Italy;*
[2]*Dipartimento di Scienze, Università Roma Tre, Largo San Leonardo Murialdo 1, 00146, Rome, Italy;*
[3]*LaMS — Modelling & Simulation Lab, Università Roma Tre, Via Corrado Segre, 6 I-00146 Rome, Italy;*
[4]*Dipartimento di Matematica e Fisica, Università Roma Tre, Roma, Italy, Via Corrado Segre, 6 I-00146 Rome, Italy; and*
[5]*Dipartimento di Scienze della Terra, dell'Ambiente e delle Risorse, Università degli Studi Federico II, Largo San Marcellino 10, 80138 Naples, Italy*
[*]*Correspondence to be sent to: Paolo Piras, Center for Evolutionary Ecology, Largo San Leonardo Murialdo 1, 00146, Rome, Italy; E-mail: ppiras@uniroma3.it.*

Recieved 30 January 2013; reviews returned 14 May 2013; accepted 3 August 2013
Associate Editor: Norm MacLeod

Abstract.—Cat-like carnivorous mammals represent a relatively homogeneous group of species whose morphology appears constrained by exclusive adaptations for meat eating. We present the most comprehensive data set of extant and extinct cat-like species to test for evolutionary transformations in size, shape and mechanical performance, that is, von Mises stress and surface traction, of the mandible. Size and shape were both quantified by means of geometric morphometrics, whereas mechanical performance was assessed applying finite element models to 2D geometry of the mandible. Additionally, we present the first almost complete composite phylogeny of cat-like carnivorans for which well-preserved mandibles are known, including representatives of 35 extant and 59 extinct species of Felidae, Nimravidae, and Barbourofelidae. This phylogeny was used to test morphological differentiation, allometry, and covariation of mandible parts within and among clades. After taking phylogeny into account, we found that both allometry and mechanical variables exhibit a significant impact on mandible shape. We also tested whether mechanical performance was linked to morphological integration. Mechanical stress at the coronoid process is higher in sabertoothed cats than in any other clade. This is strongly related to the high degree of covariation within modules of sabertooths mandibles. We found significant correlation between integration at the clade level and per-clade averaged stress values, on both original data and by partialling out interclade allometry from shapes when calculating integration. This suggests a strong interaction between natural selection and the evolution of developmental and functional modules at the clade level. [Comparative methods; felidae mandible; finite element analysis; geometric morphometrics; morphological integration; sabertooth; structural performance]

Understanding phenotypic evolution is a central topic in evolutionary biology. Phenotypes reflect multiple selective pressures that operate at multiple scales: from the individual to the species (e.g., developmental and mechanical constraints, key innovations). The term "phenotype" may refer to the morphology of biological structures, to their mechanical performance, or to the organization of their constitutive parts, that is, morphological integration. These three attributes define how phenotypes come about, change through a lineage's history, and work, in the light of adaptation and as conditioned by phylogenetic effects.

In this regard, the mammalian mandible has received great interest for its obvious role in a primary organismal function (feeding) (Herring 1980, 1993). From an adaptationist perspective, mandibular geometry should just reflect its performance in chewing and grappling of food. However, early attempts to explain the variation in mandible geometry among mammals suggest that evolutionary changes among major clades explain more variation than does niche differentiation *per se* (Crusafont-Pairó and Truyols-Santonja 1956, 1957, 1958). This has been recently confirmed for two different mammalian groups: Carnivora (Meloro et al. 2008; Meloro and O'Higgins 2011) and Ungulates (Raia et al. 2010). Although a phenotype's value as an adaptation must be studied in terms of its performance, this was rarely applied to the mammalian mandible (cf. Therrien 2005a,b; Wroe et al. 2007; Tseng and Binder 2009).

In this article, we studied the relationships between morphological variation in mandible geometry, the mandible's structural performance in response to bite solicitation, and its morphological integration as conditioned by phylogenetic effects. Our study model includes all the cat-like carnivorans: members of the suborder Feliformia (the subfamilies Felinae and Machairodontinae, within Felidae), and of the families Nimravidae and Barbourofelidae.

Cats are and always were unambiguously strict meat eaters (Ewer 1973; Therrien 2005b; Van Valkenburgh 2007; Christiansen 2008; Slater and Van Valkenburgh 2008; Van Valkenburg and Wayne 2010; Meloro and Slater 2012). The homogeneity in cat-like carnivorans feeding habitus is reflected in their dentition, which is optimally designed for slicing meat and severing tendons. The lower carnassial (m1) shows a reduction in the posterior cusps (hypo and entoconid). The lower premolar row is generally short and separated from the canine by a diastema. Interestingly, these adaptations (which occurred iteratively among hypercarnivorous carnivorans, Holliday and Steppan 2004) did not prevent ecomorphological differentiation

among cats: some species developed extremely long upper canines (Turner and Antón 1997; Feranec 2008) allowing for the occupation of a distinct (and now extinct) predatory niche: the sabertooth. Therrien (2005b) and Christiansen (2008) showed that the sabertooth mandible is unique in shape. It has shorter ramii, longer diastema, and deep mandibular flanges (Prevosti et al. 2010) as compared with the mandible of conical toothed cats. These adaptations are related to the elongation of the upper canines, and allow a wide jaw gape (Andersson et al. 2011; Figueirido et al. 2011). Although the sabertooth's ecomorphology (and how it differs from conical-toothed cats) has attracted so much interest, it is still unclear how the two major cat-like carnivoran morphotypes (i.e. conical-toothed cats and sabertooth) differ in ecomorphology, and if the convergence of different lineages on sabertoothedness did lead to truly equivalent performances. For instance, Therrien (2005b) argued that sabertooths delivered a strong and powerful bite, whereas McHenry et al. (2007), by applying finite element analysis (FEA) to skulls, suggested that bite force in *Smilodon* (the epitome of sabertoothedness) was lower than in a similarly sized lion. Furthermore, the famed sabertooth canines occur in either one of two different kinds, the shorter dirk-tooth with crenulations on the margins, as in the genus *Homotherium*, and the overly long canines of cats such as *Smilodon*, which have smooth margins (Turner and Antón 1997).

Recent advancements in the study of skull geometry and biomechanical modelling (Pierce et al. 2008) suggest that combining geometric morphometrics (GM) and FEA provides the best insight about the mechanical performance of skeletal elements in relation to their geometry (Piras et al. 2012b). Additionally, Klingenberg (2010), Monteiro and Nogueira (2010) and especially Meloro et al. (2011) and Meloro and Slater (2012) introduced a new way to interpret interspecific shape variation by looking at functional covariation between anatomical districts, such as the corpus and the ramus in the mandible, or the rostrum and the braincase in the skull.

Several works focused on mandible morphology and/or integration in a number of different species (Prevosti et al. 2010; Meloro et al. 2011; Meloro and Slater 2012). Others focused on the structural performance of cranio-mandibular structures (McHenry et al. 2007; Christiansen 2011). However, few studies have linked integration to mechanical performance in mandibles. Doing so would allow a test of the hypothesis that morphological integration varies as a response to mechanical solicitations (Monteiro and Nogueira 2010). We hypothesized that morphological integration between distinct mandibular parts (the corpus that holds the teeth and the ramus where masticatory muscles attach) is stronger in the more "extreme" phenotypes (e.g. taxa showing a relatively longer upper canine, the sabertooths) in order to face stronger mechanical solicitations. We combined GM and FEA to study the most comprehensive data set of cat-like species mandibles (inclusive of extant and extinct species) ever assembled, in order to test if and how mechanical performance between conical and sabertoothed species differs. We also provide a deeper look into the sabertooth morphology, testing quantitatively if sabertooths represent a single ecomorphology (Meachen-Samuels 2012), or they are better ascribed to distinct ecomorphologies (Martin et al. 2000). As sabertoothedness evolved in different lineages of Carnivora, we tested if phylogenetic signal in mandible shape is present in our mandible data set. We predicted lower signal in groups with higher morphological integration and mechanical performance. To test these hypotheses, we introduce a new comprehensive phylogeny of cat-like carnivorans, including nearly all of the extant felids and most extinct cat-like carnivorans for which sufficiently well-preserved mandibles were available.

Materials and Methods

Material

We collected digital pictures of hemi-mandibles in lateral view, belonging to 726 different individuals, from both original photographs and published pictures. Online Appendix I (available from Dryad data repository; doi:10.5061/dryad.kp8t3) reports the specimen list and the number of individuals per species. We used a standard protocol to take pictures at a distance of 2 m, in order to minimize distortion due to parallax (cf. Mullin and Taylor 2002; Meloro et al. 2008; Meloro et al. 2011). Our sample includes 94 species: 35 extant and 59 extinct. Out of 37 extant felids, 35 were included in our study. The two species we missed are *Pardofelis badia* and *Leopardus jacobita*. For extinct Felidae, we included every extinct species assigned to the families Barbourofelidae and Nimravidae for which at least one complete mandible was available in the museum collections we visited, or in the literature (full list in Online Appendix I available from Dryad data repository; doi:10.5061/dryad.kp8t3).

GM

We recorded 10 landmarks and 27 semilandmarks on the hemi-mandible of each specimen using the software tpsDig 2.16 (Rohlf 2010a) (Fig. 1). The landmark digitalization was performed by one of us (L.M.) to minimize interobserver error whereas intraindividual digitalization error was assessed using standard protocols (Cardini and Tongiorgi 2003; Meloro 2011). Measurement error for interlandmark distances was always lower than 5%, on original, as well as on published, pictures. The semilandmarks were automatically recorded at equal distances along curves that we drew on the pictured specimens by using tpsDig 2.16. Semilandmarks are useful to depict the shape of curved lines where landmarks cannot be detected. It is assumed that contours are homologous

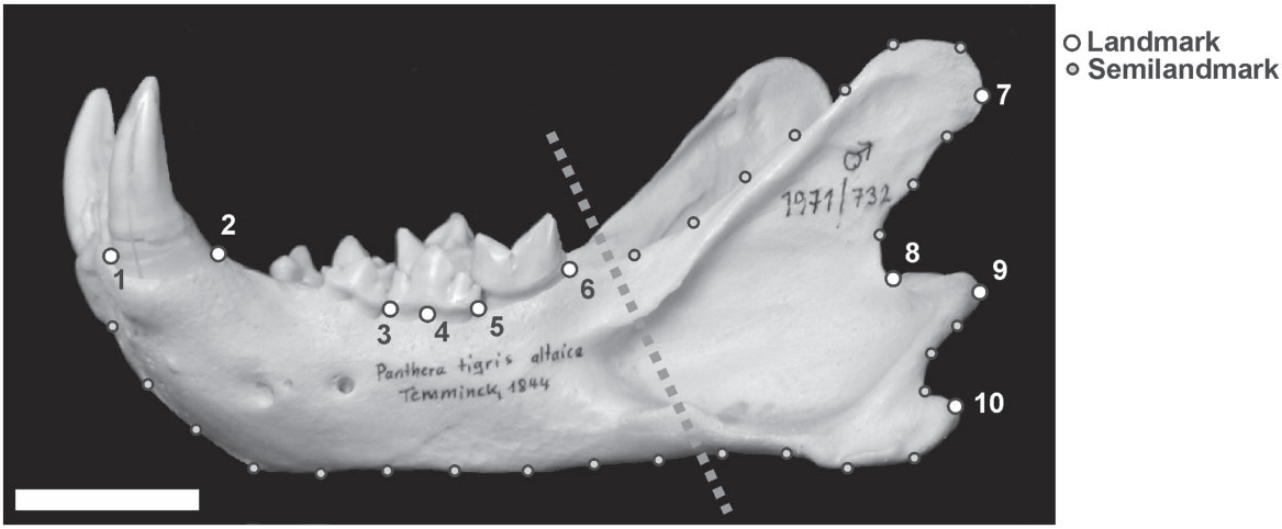

FIGURE 1. Landmarks and semilandmark configuration applied to a *Panthera leo* left hemimandible. Landmark definitions: 1) anterior tip of canine alveolus; 2) posterior tip of canine alveolus; 3) posterior of p4 alveolus; 4) spine of p4 alveolus; 5) posterior tip of p4 alveolus; 6) posterior tip of m1 alveolus; 7) posterior tip of coronoid process; 8) maximum curvature between articular process and ascending ramus; 9) posterior tip of condyloid process; 10) posterior tip of angular process. The two mandibular modules (the corpus and the ramus) are identified by dotted line. The white scale bar is 5 cm long.

among specimens, whereas their individual points need not be (MacLeod 1999; Bookstein 1997; Bookstein et al. 2002).

Generalized procrustes analysis (GPA; Bookstein 1991, Goodall 1991) was used to extract shape variables from the raw landmark and semilandmark coordinates. GPA rotates, aligns, and scales landmark configurations to unit centroid size (CS = the square root of the sum of squared distances of a set of landmarks from their centroid; Bookstein 1986) so that shape differences between specimens are not due to rotation, position, and size (Rohlf and Slice 1990).

As semilandmarks differ from landmarks, these points, in addition to being optimally translated, rotated, and scaled, are slid along the contour until they match, as much as possible, the positions of corresponding points along the contour in the reference configuration (Adams et al. 2004; Perez-Bernal et al. 2006). All GM analyses were performed using the R package "Morpho," Schlager (2013). This package minimizes the Bending Energy during the sliding process.

After GPA, Procrustes coordinates of different individuals belonging to a single species were averaged as to obtain 94 different coordinates, taken as the shape variables. Principal component analysis (PCA) was performed on Procrustes coordinates to find orthogonal axes of maximal variation. This is a common procedure in geometric morphometric studies (Adams et al. 2004; Claude 2008; Figueirido et al. 2010).

Phylogeny

We built a composite phylogeny (using Mesquite 2.73, Maddison and Maddison 2010) that included all species present in our data set. The phylogeny is based on published cladistic analyses of extinct and extant taxa, and on their stratigraphic range. The phylogenetic tree adopted in our study is presented in Figure 2. Five monophyletic groups of cat-like carnivorans are traditionally identified: 1) Barbourofelidae, 2) Felinae, 3) Machairodontinae and a distinct clade including 4) *Hyperailurictis+Nimravides* within Felidae, and 5) Nimravidae (Peigné 2003; Morlo et al. 2004; Werdelin et al. 2010). We followed Peigné (2003) for the affinities between Nimravidae and the Felidae+Barbourofelidae group, and for the phylogenetic relationships within Nimravidae. Geraads and Güleç (1997), Morlo et al. (2004), Tseng et al. (2010), and Werdelin et al. (2010) were considered for the phylogenetic relationships within Barbourofelidae. *Haplogale media* and *Proailurus lemanensis* are considered basal taxa to Barbourofelidae and Felidae, respectively, in keeping with Werdelin et al. (2010). For the phylogenetic relationships within *Hyperailurictis+Nimravides*, we followed de Beaumont (1990), Rothwell (2003), and Werdelin et al. (2010). *Pseudaelurus quadridentatus* is herein considered a basal machairodont (Werdelin et al. 2010), whereas the relationships within machairodonts are based on Kurtén and Anderson (1980), Werdelin and Lewis (2001), Andersson and Werdelin (2005), Werdelin and Peigné (2010), and Werdelin et al. (2010). *Styriofelis* is the sister group to Felinae (Werdelin et al. 2010). Inner phylogenetic relationships within Felinae follow Johnson et al. (2006) and Werdelin et al. (2010). We partially had to recalibrate the branch lengths in the molecular phylogeny proposed by Johnson et al. (2006) after adding some extinct taxa (e.g., *Pristifelis attica*, *Felis christoli*, *Miracinonyx* spp., and *Panthera* spp.). Further details about the systematics arguments upon which we built our phylogeny, and additional literature sources are available as Online Appendix II (available from Dryad data repository; doi:10.5061/dryad.kp8t3).

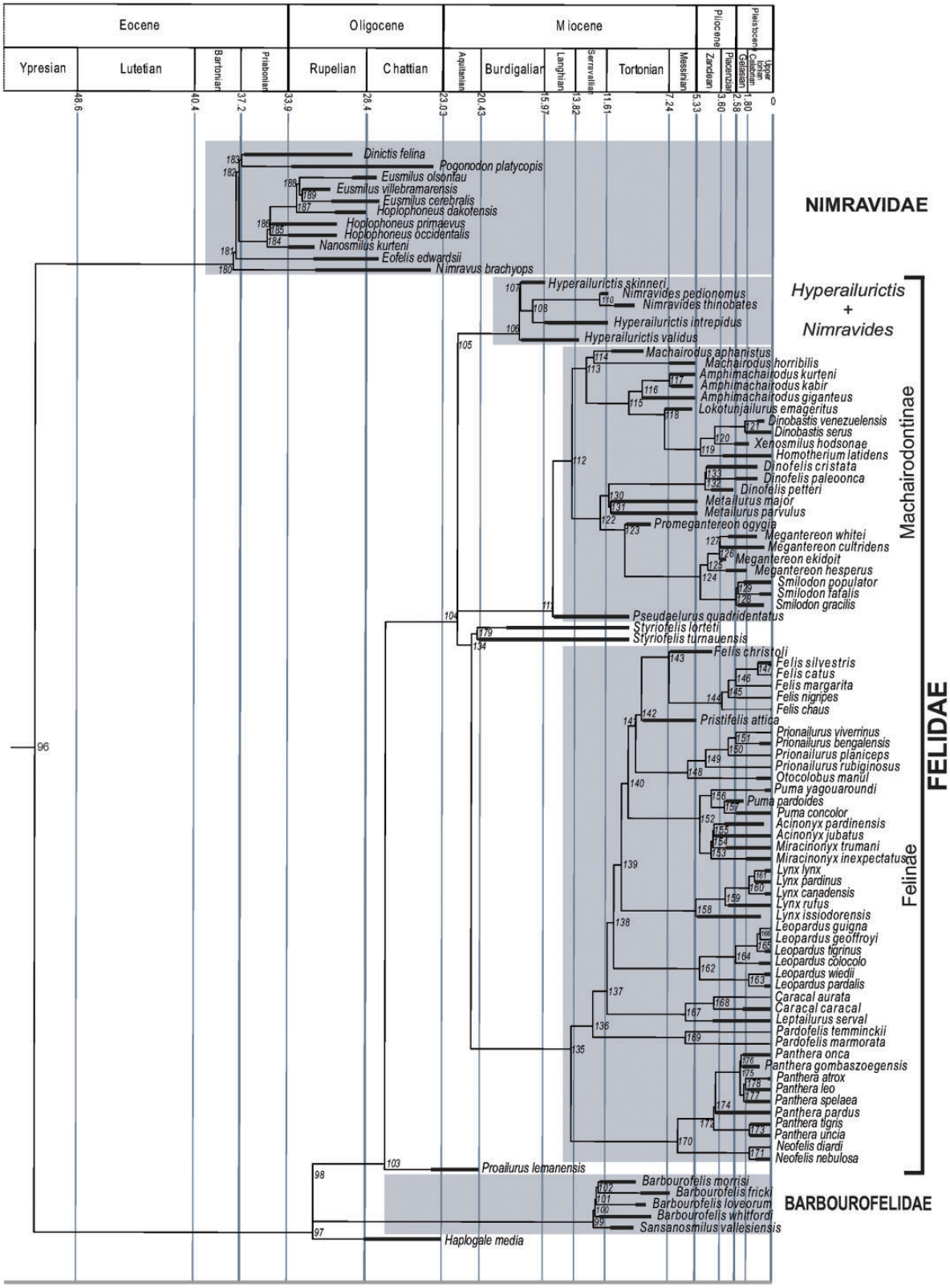

FIGURE 2. Phylogenetic tree comprehensive of all species considered in this work. Thicker lines indicate the observed stratigraphic range of taxa.

Morphological Integration

Several studies have examined morphological integration within the mammalian mandible (Atchley et al. 1982; Atchley and Hall 1991; Cheverud et al. 1991, 1997, 2004; Atchley 1993; Badyaev and Foresman 2000, 2004; Klingenberg and Leamy 2001; Klingenberg et al. 2001, 2003, 2004; Leamy et al. 2002; Ehrich et al. 2003; Cheverud 2004; Badyaev et al. 2005; Polly 2005; Márquez 2008; Klingenberg 2009; Zelditch et al. 2009) by exploring different modular hypotheses. Here we adopt the same modular hypothesis of Meloro et al. (2011) in order to compare, among clades, the degree of morphological integration between the corpus, which houses the teeth and provides attachment for some of the jaw-closing muscles, and the ramus, which articulates with the cranium and provides attachment sites for the most prominent jaw-closing muscles. Although this distinction is clearly functional, it also reflects the pattern of aggregation of mesenchymal cells during embryonic development, which condense to form the morphogenetic units of the developing mandible (Atchley and Hall 1991).

We used the *RV* coefficient (Escoufier 1973) as a metric of covariation between the various sets of shape variables (calculated using the function RV.rtest() in R package "ade4," Dray and Dufour 2007). This coefficient was originally proposed by Escoufier (1973) as a measure of the association between two multivariate sets of data. The *RV* coefficient is analogous to the R-square in the univariate case (Claude 2008). The equation for calculating *RV* therefore represents the amount of covariation scaled by the amount of variation within the two sets of variables, which is analogous to the calculation of the correlation coefficient between two variables (Klingenberg 2009). *RV* may take any value from 0 to 1.

First, we explored global morphological integration, pooling the entire sample. Partial least square (PLS) analysis was also employed to visualize the covariation between corpus and ramus at the macroevolutionary scale (cf. Meloro et al. 2011; Meloro and Slater 2012). This exploratory technique identifies the vectors (Singular Warps) that maximise co-variation between two blocks of multivariate data (Rohlf and Corti 2000) that in our case are represented by shape variables of the corpus and ramus modules, respectively. We then repeated the analysis of morphological integration (*RV* coefficient) by multiplying shape variables by the inverse of the phylogenetic covariance matrix, in order to factor out data nonindependence due to phylogeny. We performed these analyses using the function oscorespls.fit () in R package "pls" (Mevik and Wehrens 2007). A similar procedure was applied in Piras et al. (2012a).

We also evaluated which modulus is more correlated with mechanical stress affecting the entire mandible by means of multivariate regression, using Procrustes Coordinates as dependent variables matrix and stress variables as the independent variable. The *RV* coefficient was computed for each of the five main clades in our phylogeny to relate it with the per-clade averaged biomechanical variables (see below).

FEA

In order to reconstruct the mandibular geometry, we used Procrustes coordinates as control points to generate a smooth, closed contour by spline approximation using a Matlab routine available in Online Appendix III (available from Dryad data repository; doi:10.5061/dryad.kp8t3). The reconstructed geometry is then used as a 2D computational domain where a structural problem in the plane stress regime is posed; the problem is solved by means of FEA using the commercial software COMSOL Multiphysics 4.2 (http://www.comsol.com). FEA is a mathematical framework that provides a quantitative evaluation of the strain and stress state within a solid with given material properties, under appropriate applied loads and boundary conditions that mimic a particular functional or behavioural scenario (Rayfield 2007, 2011).

These results yield a thorough characterization of the mechanical state of the structure (see also Richmond et al. 2005; Zienkiewicz et al. 2005). A similar procedure, that is, creating finite element models starting from GM data, was successfully applied by Young et al. (2010), Pierce et al. (2008, 2009a, 2009b), and Stayton (2009) among others.

Here, we used FEA in a comparative, rather than validative, fashion. One of the key questions in modern biologically oriented finite element studies is the reliability of simulation in comparison with real experimental studies. Many studies (Ross et al. 2005; Strait et al. 2005; Kupczik et al. 2007; Farke 2008; Gröning et al. 2009; Rayfield 2011) focused on this problem, demonstrating that incorporating more precise approximation in finite element simulations (anisotropic material properties, muscle activation data, etc.) improves the correlation between simulations and real experimental results. We applied the same comparative approach for all finite element models, with our objective to compare the mandibular mechanical performance of species in the context of their phylogenetic relationships. Isotropic material properties corresponding to bovine haversian bone (Young's modulus: 10 GPa, Poisson's ratio: 0.41, Rayfield et al. 2001) were assumed for all the models in our study.

Having used Procrustes coordinates to build our geometries, we rescaled them to the same size unit, thereby partialling out any evolutionary allometric effect among species in estimating the mechanical performance variables (see below).

Our structural model of the mandible works according to a pressure load (i.e., a force per unit area) applied on the base of the canine alveolus, which simulates bite force. The mandible model has an elastic constraint at the ascending ramus. Due to the high morphological variability of the mandible among felids, nimravids, and barbourofelids, two different constraints were

in fact considered: The first was placed on the posterior border of the coronoid process, where the temporalis muscle inserts from the temporalis area, the second was placed on the condyloid process and on the angular process, where the masseter+pterygoid muscular complex inserts from the zygomatic area. Finally, all the remaining portions of the boundary have a free boundary condition.

Due to the impossibility of applying the dry skull method (Thomason 1991) for all our 94 species to obtain bite forces for both extant and extinct species (cf. Wroe et al. 2005; Sakamoto et al. 2010) we used the estimated bite force of *Smilodon fatalis* computed by Sakamoto et al. (2010) placed at the canine.

In order to obtain realistic results (in terms of absolute magnitude), we scaled bite force according to the actual size of our geometries as obtained from Procrustes coordinates. Due to the purely comparative approach we applied, scaling has no direct effect on our results. This means that using a different bite force returns just differently scaled results.

Figure 3a shows the 2D geometry used to solve the structural problem, the portion of the boundary with the applied biting load, and the portion with the elastic constraints. The beam theory, using the theory of elasticity (Timoshenko 1922), can give a useful estimate of the distribution of the reaction forces along the ascending ramus of the mandible. We begin with the simple scheme in Figure 3b: The bite force f is balanced by a reaction force f, and a reaction torque $c = lf$, proportional to the distance l between the bite force and the point we consider at the vertical ramus. Then, the schemes in Figure 3c,d are used to calculate the normal stress σ and the shear stress τ along the vertical ramus, assuming this ramus to have a simple rectangular cross section, with height h, width b (in plane-stress analysis it is assumed to be unitarian), and moment of inertia $I = bh^3/12$. Figure 3e shows an actual mandible of an extant felid (*Panthera leo*). Beam theory predicts the normal stress σ to be linear along the height, and the shear stress τ to be quadratic; denoted with y (the vertical coordinate of any geometry). With $y = 0$ at the center of the vertical ramus, we may write:

$$\sigma(y) = c/I\, y, \tau(y) = 6f/(bh^3)(h^2/4 - y^2) \quad (1)$$

Thus, the normal stress is maximal at the ends, $\sigma_{max} = \sigma(h/2) = 6c/(bh^2)$, whereas the shear stress is maximal at center, $\tau_{max} = \tau(0) = 3f/(2bh)$. Fixing the dorsoventral height of the beam, both formulas yield higher stress values for those species having a shorter vertical ramus.

To asses the estimates given by the beam theory, we use FEA to compute the actual stress states in our models. Denoting with x, y the horizontal and vertical coordinates, the stress tensor S is represented by the 2×2 matrix:

$$S = \begin{bmatrix} S_x S_{xy} \\ S_{xy} S_y \end{bmatrix}$$

The corresponding Von Mises stress is given by:

$$\sigma_M = (S_x^2 + S_y^2 - S_x S_y + 3S_{xy}^2)^{1/2}.$$

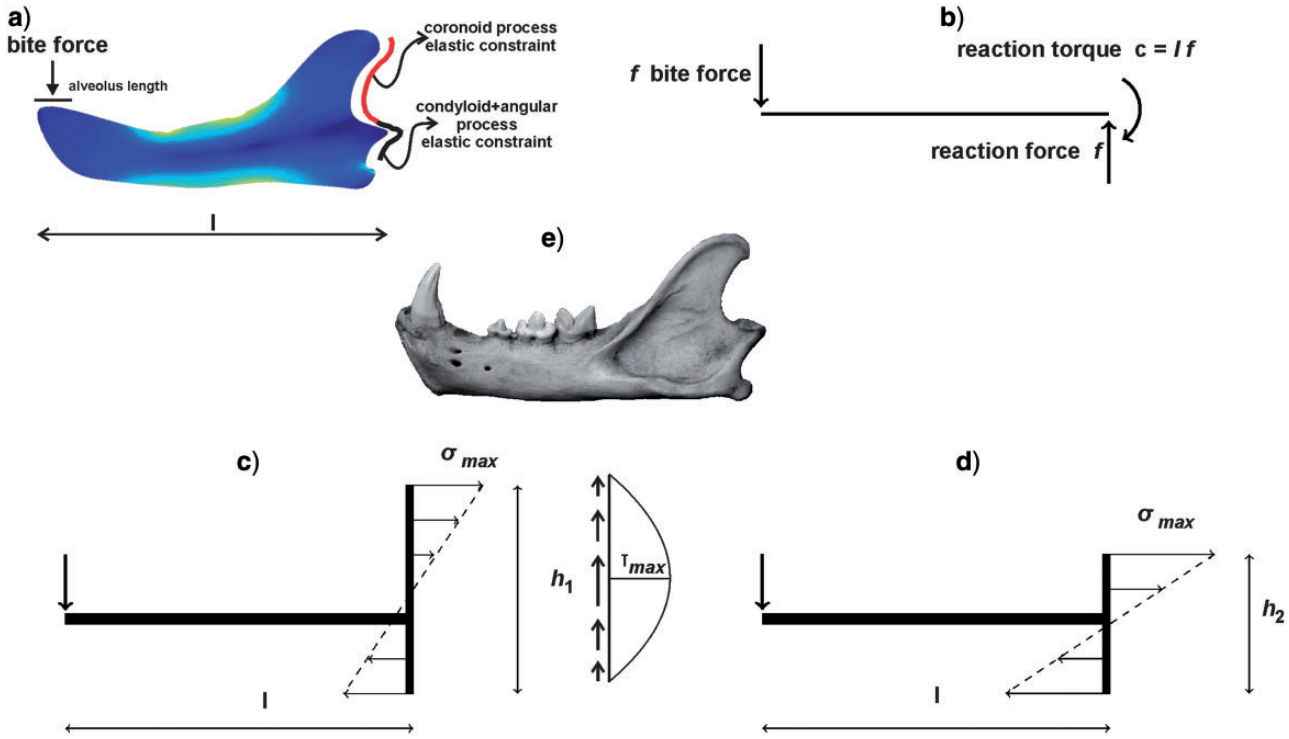

FIGURE 3. Structural model used for our simulations. a) Finite Element Model. b) 1D scheme showing forces acting on the mandible corpus. c) and d) Diffrences in σ due to different height of ascending ramus. e) Picture of *Panthera leo* mandible.

The x and y components of the reaction acting along the ascending ramus of the mandible are given by:

$$t_x = S_x n_x + S_{xy} n_y, t_y = S_{xy} n_x + S_y n_y,$$

where n_x, n_y are the components of the unit normal vector to the boundary.

The beam theory predicts a stress state given by:

$$S = \begin{bmatrix} \sigma\tau \\ \sigma 0 \end{bmatrix}$$

with σ and τ as above; thus, the corresponding Von Mises stress:

$$\sigma_{Mbt} = (\sigma^2 + 3\tau^2)^{1/2} \quad (2)$$

We can compare the Von Mises stresses σ_M and σ_{Mbt}.

Following our model (depicted in Fig. 3a) beam theory and FEA predict that von Mises stress is positively related to bite force, and then to the reaction (a surface traction), once the dorsoventral height of horizontal ramus has been fixed.

In fact, from equation (1) and equation (2) it follows:

$$\sigma_{Mbt}(x,y) = 3/2f/(bh^3)[64x^2y^2 + 3(h^2 - 4y^2)^2]^{(1/2)}.$$

We used global von Mises stress calculated on the whole mandible area and the maximum surface traction calculated along the constrained posterior boundaries as structural variables to be used in subsequent comparative analyses.

Linear Models and Comparative Methods: Phenotypic Differences Between Clades

We accounted for the the potential effects of shared ancestry on the interspecific phenotypic variables. First, we tested for significant phylogenetic signal in both stress variables and in CS by estimating the K statistic (Blomberg et al. 2003), using the function phylosig() in the R package "phytools" (Revell 2012). Second, we used fitContinuous() function in "GEIGER" (Harmon et al. 2008) in order to find out which evolutionary model is most supported. The best model's parameter estimates were used to transform the tree branch lengths in order to provide the most appropriate covariance matrix for the residuals in univariate phylogenetic GLS analyses, and in phylogenetic ANOVAs (Revell 2010, see below).

The seven models tested are Brownian motion which is a random walk with constant variance; Ornstein-Uhlenbeck (which fits a random walk with a central tendency with an attraction force proportional to the parameter alpha); Pagel's lambda (which provides a tree branch length transformation as to maximize the fit to Brownian motion); Pagel's kappa (which tells if evolution either concentrates at nodes or is proportional to branch lengths as in the Brownian motion); Pagel's delta (which tells if the rate of evolution changes in time); ACDC model (which fits an exponential change to the rate of evolution through time); and, finally, the white noise model (which assumes no phylogenetic signal is present in the data). The Akaike Information Criterion (AIC) was used to find the best-fit model for character evolution.

Shape is multivariate, so we could not estimate Pagel's lambda or Blomberg's K statistics to test for phylogenetic signal in the data. Instead, we tested the presence of a phylogenetic structuring in the data by performing a Mantel test between a Procrustes distance matrix and a patristic distances matrix coming from our phylogeny.

Then, we tested for differences in shape, stress variables and size between the five distinct clades identifiable in our tree: Felinae, Barbourofelidae, Machairodontinae, *Hyperailurictis+Nimravides* and Nimravidae. To this aim, we performed phylogenetic ANOVA (using stress variables and size as dependent variables, respectively) and phylogenetic MANOVA (using shape data as dependent variables) using the five clades as a factor. Pairwise comparisons were made using "phy.anova" and "phy.manova" functions available in GEIGER R package (Harmon et al. 2008).

Regression Models and PGLS

We accounted for the relationships between shape, size, and stress variables by using linear models taking phylogenetic relationships into account. We achieved this by adopting the phylogenetic generalized least squares (PGLS) regression (Rohlf 2001, 2006). This method is equivalent to the phylogenetic independent contrasts (PIC) first proposed by Felsenstein (1985). Standard regression methods assume data independence. Due to phylogenetic relationships, multispecies biological data rarely meet this condition. Taking phylogeny into account in regression allows reducing standard error due to nonindependence caused by shared ancestry over a model that neglects phylogeny (Felsenstein 1985; Garland 1992; Garland et al. 2005). In order to evaluate the amount of shape explained by functional demands (i.e. mechanical performance), we regressed shape data (as dependent) on stress variables (as independents).

The influence of allometry on shape or stress data was also assessed in regression models using shape data or stress variables as dependents, and size as independent. All these models were performed by using PGLS analyses and performed in R using the function genpgls() written by one of the authors (PP; it can be found in Online Appendix IV, available from Dryad data repository; doi:10.5061/dryad.kp8t3). Our stress data were calculated using shapes scaled to unit size, that is, using Procrustes coordinates and by applying the same loading (=bite force) at canine to all finite element models. Of course, a small domestic cat does not have the same bite force as a lion but their mandibular shapes are quite similar in comparison with a *Smilodon*. Thus, evolutionary allometry (=the allometry that occurs between approximately equally aged individuals of different species) must be controlled when testing the performance of different shapes (Dumont et al. 2009;

Slater et al. 2009; Slater and Van Valkenburgh 2009). For this reason we used Procrustes coordinates that are all scaled to unit size. However, we verified the impact of scaling by exploring the relationship among stress variables and between stress variables and shape by re-multiplying stress data by individual-specific CS. With this procedure, bite forces are scaled for any individual body size (i.e. CS). In fact, we statistically confirmed that standardized bite force scales almost isometrically with standardized body mass ($\beta = 0.93$; $P = 2.2e{-}16$) as expected (Wroe et al. 2005; Sakamoto et al. 2010). We confirmed this by verifying that for those species for which Sakamoto et al. (2010) report mean body mass, our per-species averaged CS predicts species mean body mass very strongly ($R^2 = 0.94$; $P = 2.2e{-}16$).

Prior to exploring univariate relationships (i.e. between stress variables and size in ANOVAs and in univariate PGLS), we transformed the phylogenetic tree according to the most supported mode of character evolution as indicated by applying the fitcontinuous() function. For multivariate data this is not allowed and the tree was not transformed when shape entered the analysis (i.e. in MANOVAs and in multivariate PGLS), which means assuming *de facto* a Brownian motion model of evolution (Blankers et al. 2012).

Biomechanical Performance and Integration

As pointed out above, von Mises stress is proportional to surface traction and inversely related to the dorsoventral height of the geometry. On the other hand, surface traction is inversely related to the height of constrained boundaries that are placed on the ascending ramus. Thus, we first compared the predicted relationship between von Mises stress and surface traction with the observed correlation between these two variables. In fact, mandible geometry varies in both the height of mandibular corpus and in the height of the ascending ramus (and consequently in areas). Thus, the two modules vary (and possibly co-vary), and this variation differently constrains both von Mises stress and surface traction. We test here if the variation in mandibular corpus changes the predicted formal relationship between von Mises stress and surface traction. In order to do this, we performed linear regressions between observed von Mises stress and surface traction and between von Mises stress and the areas of the two functional modules defined above (calculated on the polygons identified by Procrustes coordinates of corresponding landmarks—as stress variables were calculated on these coordinates, rather than on original data—). This way we can determine if any deviation from the predicted relationship between von Mises stress and surface traction is due to differential, and possibly covarying, changes in the morphology of single modules.

We also test the hypothesis that sabertooth morphology implies covarying arrangements in the ascending ramus and mandibular corpus, thus making the integration between these two subunits stronger in sabertoothed than in conical-toothed cats. To this aim, we regressed clades' *RV*s on the per-clade averaged values of the stress variables. This allows us to verify if the morphological integration at the clade level can be interpreted as a compensation of the change in biomechanical performance due to the particular shape evolved in such group.

Again, allometry could influence such analysis at two levels. The first level is the *intra*clade allometry that could influence the calculation of *RV* coefficient. The second level is the *inter*clade allometry, that is, that due to mean size differences between clades. In order to partial out both forms of allometries, we re-computed *RV*s using residuals coming from per-clade separated regressions between shape and size and successively tested if per-clade averaged stress data or clades *RV*s were correlated with per-clade averaged size values.

Results

GM

The first 13 principal components explain 95% of total shape variance. Figure 4a,b shows the relationships between PC1 (39.74% of the total shape variance) and PC2 (17.79% of the total shape variance) and between PC1 and PC3 (12.43% of the total shape variance). Positive PC1 scores are associated with a relatively thicker mandibular corpus, a short coronoid process, a caudally expanded condyloid process, fourth premolar (p4)-first molar (m1) closer to the coronoid process than anterior symphysis, a highly developed mandibular flange expanded ventrally behind upper canines. This morphology is typical of the Barbourofelidae. Negative PC1 scores are associated with a mandibular corpus that is relatively slender, long coronoid process, short condyloid process, p4-m1 closer to the anterior symphysis than to the coronoid process, and absence of the mandibular flange. This morphology is evident in modern Felinae. Positive PC2 scores are associated with a long and thick mandible, a dorso-caudally expanded coronoid process, and a mandibular flange slightly extended ventrally. Negative PC2 scores are associated with a long and slender mandible, a coronoid process expanded dorsally, and a slender symphysis with no flange. Along PC3, major shape differences occur in the angular process, coronoid process, and relative height of the corpus and mandibular flange.

Figure 5a shows the morphological variation in mandible shape associated with CS for the entire shape, and for single modules. At high CS values the mandible is thicker behind the corpus, with a short coronoid process, a caudally extended condyloid process, an expanded canine-p4 area and a higher mandibular flange. This morphology corresponds to barbourofelids and some machairodonts. At low CS values the mandible is relatively slender, with a long coronoid process, a short condyloid process, short distance between canine and p4

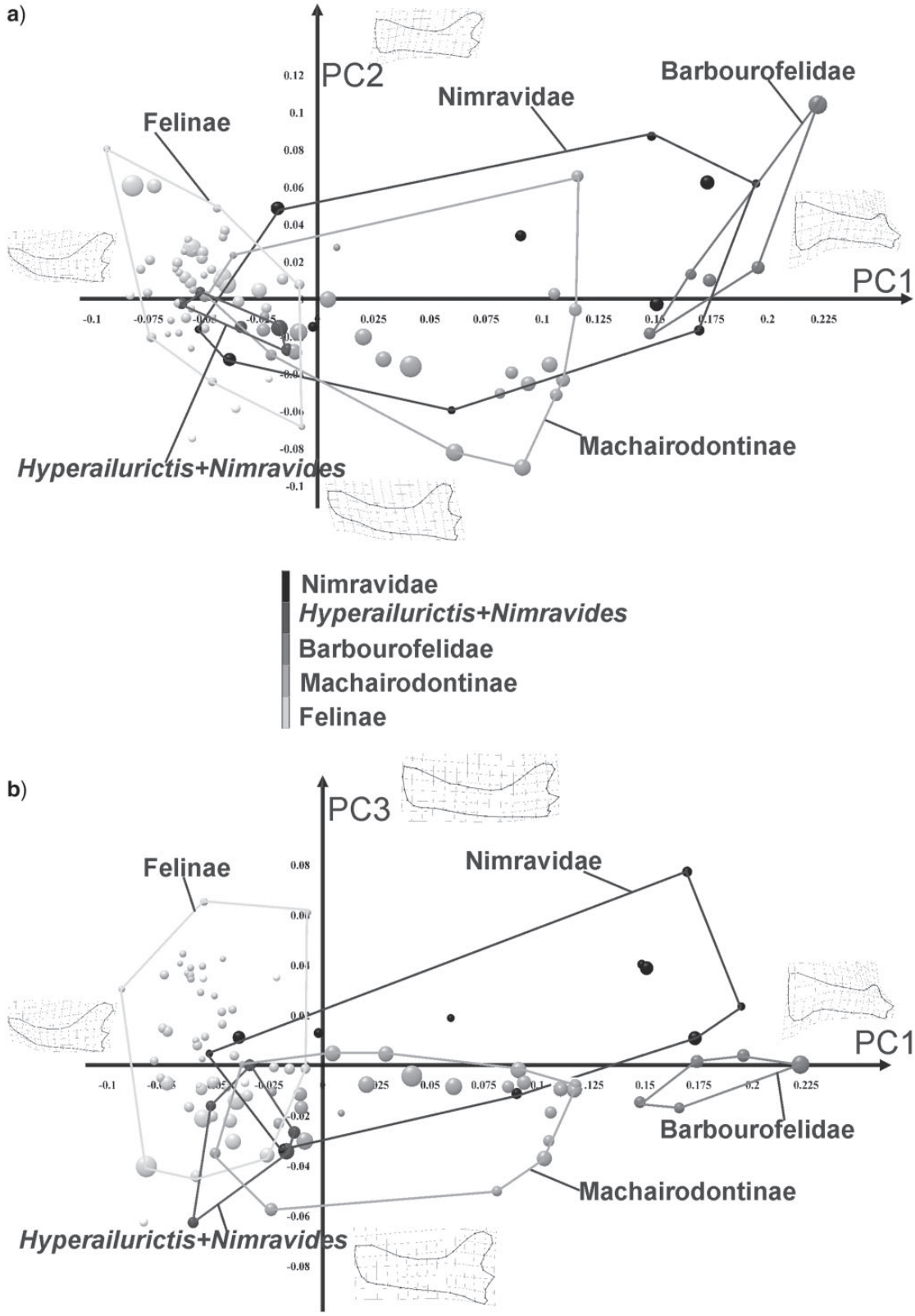

FIGURE 4. a) Relationship between PC1 and PC2; b) Relationship between PC1 and PC3. Points dimension is proportional to species mean CS.

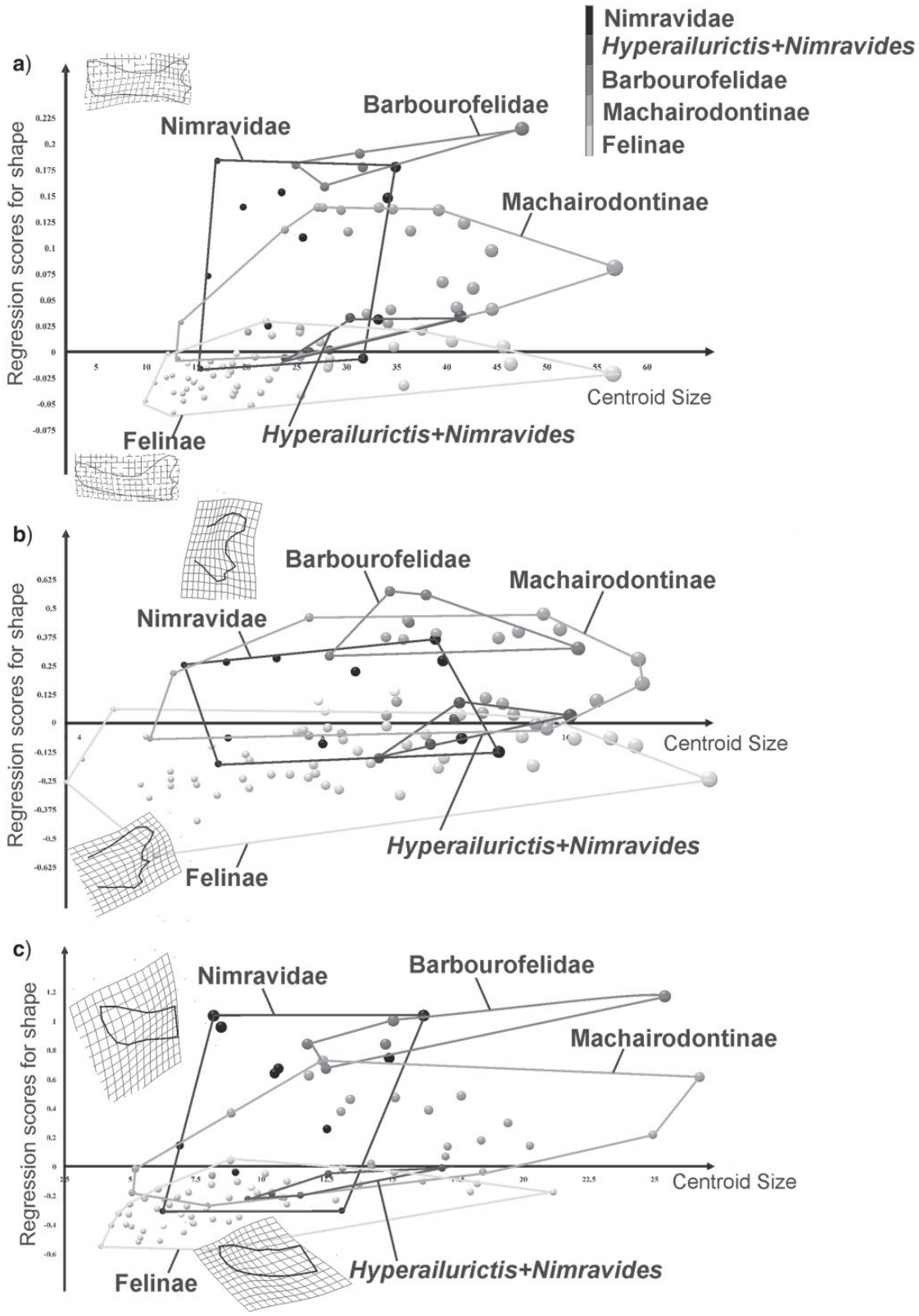

FIGURE 5. a) Morphological changes in mandible shape associated to CS. b) The same relationhip for ascending ramus. c) The same relationship for mandibular corpus. Points dimension is proportional to species mean CS.

and no mandibular flange. This structural arrangement is typical of modern felids.

Figure 5b,c show allometry related to single modules. The ascending ramus of the mandible was *less* influenced by CS than the corpus. Table 1 reports R^2 and *P*-values for individual clades for entire shape and single modules. PGLS was performed only on the pooled data set (i.e. on the entire phylogeny).

Morphological Integration

Table 2 reports *RV* coefficients for the pooled sample and the five main clades of our phylogeny. All *RV*s are significant except for the *Hyperailurictis+Nimravides* clade. This could be due to the low number of taxa (only five species) in this clade. Barbourofelidae appears to be the clade with the highest degree of morphological integration, followed by Nimravidae and Machairodontinae. Felinae is the least-integrated clade. *Hyperailurictis+Nimravides* constitute an outlier in this distribution having a *RV* coefficient slightly larger than in machairodonts. Pooled *RV* calculated on phylogenetic transformed data was significant as well (RV = 0.42; $P = 0.009$).

Figure 6 shows the morphological covariation between the two modules identified on the mandible according to non phylogenetic PLS analysis performed on the pooled sample. The first pair of singular warps (SWs) explains 98.9% of total covariance. On positive SW1 scores the coronoid process is short and massive, the condyloid process is extended caudally, and the horizontal ramus is thick with a well-developed mandibular flange, as it can be seen in barbourofelids and sabertoothed machairodonts. Negative SW1 scores correspond to a dorso-caudally expanded, high and slender coronoid process, a short condyloid process, a long and slender horizontal ramus and no mandibular flange, which is typical of Felinae.

TABLE 1. OLS for individual clades and PGLS models for pooled data set for shape-size relationships

Procrustes coordinates	CS
OLS	
Entire shape	
Nimravidae	$R^2 = 0.038$; $P = 0.79$
Hyperailurictis+Nimravides	$R^2 = 0.20$; $P = 0.48$
Barbourofelidae	$R^2 =$ **0.69**; $P =$ **0.038**
Machairodontinae	$R^2 =$ **0.11**; $P =$ **0.03**
Felinae	$R^2 =$ **0.18**; $P =$ **0.001**
Mandibular corpus	
Nimravidae	$R^2 = 0.082$; $P = 0.38$
Hyperailurictis+Nimravides	$R^2 = 0.42$; $P = 0.17$
Barbourofelidae	$R^2 = 0.69$; $P = 0.06$
Machairodontinae	$R^2 =$ **0.14**; $P =$ **0.023**
Felinae	$R^2 =$ **0.21**; $P =$ **0.001**
Ascending ramus	
Nimravidae	$R^2 = 0.07$; $P = 0.47$
Hyperailurictis+Nimravides	$R^2 = 0.19$; $P = 0.69$
Barbourofelidae	$R^2 =$ **0.57**; $P =$ **0.025**
Machairodontinae	$R^2 = 0.03$; $P = 0.66$
Felinae	$R^2 =$ **0.08**; $P =$ **0.01**
PGLS (for pooled data sets only)	
Entire shape	$P =$ **2.18*e*−6**
Mandibular corpus	$P =$ **7.74*e*−8**
Ascending ramus	$P =$ **0.04**

Significant results are shown in bold.

TABLE 2. *RV* coefficients for the pooled sample and the five main clades under study

Clade	*RV*	*P*
Pooled sample	0.64	**0.001**
Nimravidae	0.61	**0.008**
Hyperailurictis+Nimravides	0.57	0.27
Barbourofelidae	0.85	**0.003**
Machairodontinae	0.49	**0.001**
Felinae	0.25	**0.001**

Significant results are shown in bold.

FEA

Figure 7a reports the maximum surface traction experienced by some representative taxa (among the 94 analyzed) belonging to the five main clades of our phylogeny and their von Mises stress patterns. Barbourofelids and derived nimravids appear to have the smallest von Mises stress and the highest surface traction, followed by machairodontines. Felinae shows an opposite pattern in comparison with Barbourofelidae. Figure 7b,c show, respectively, the relationship between von Mises stress and surface traction predicted by beam theory when fixing beam height and that observed in experimental data. They are strikingly different given the covariation of mandible modules depicted in Figure 6. Biomechanical implications of this are described below and in the section Discussion.

Figure 7d shows the relationship between von Mises stress and surface traction after re-multiplying these variables by individual-specific CSs (see below for linear models results); the relationship is positive and significant.

Figure 8a,b,c shows the morphological changes associated with the relationship between whole mandible shape or module shapes and surface traction scores. High surface traction corresponds to short coronoid process, caudally extended condyloid process, and well-developed mandibular flanges, as seen in barbourofelids and some nimravids. When surface traction is low the mandible is long and slender, and flanges are absent. This condition is typical of modern felids. The relationship between shape and von Mises stress follows an inverse pattern (Fig. 9a) in comparison with surface traction (Fig. 8a). Yet, if von Mises stress and surface traction are both multiplied by original CS (reintroducing allometric effects), the two variables behave the same way (Fig. 9b,c).

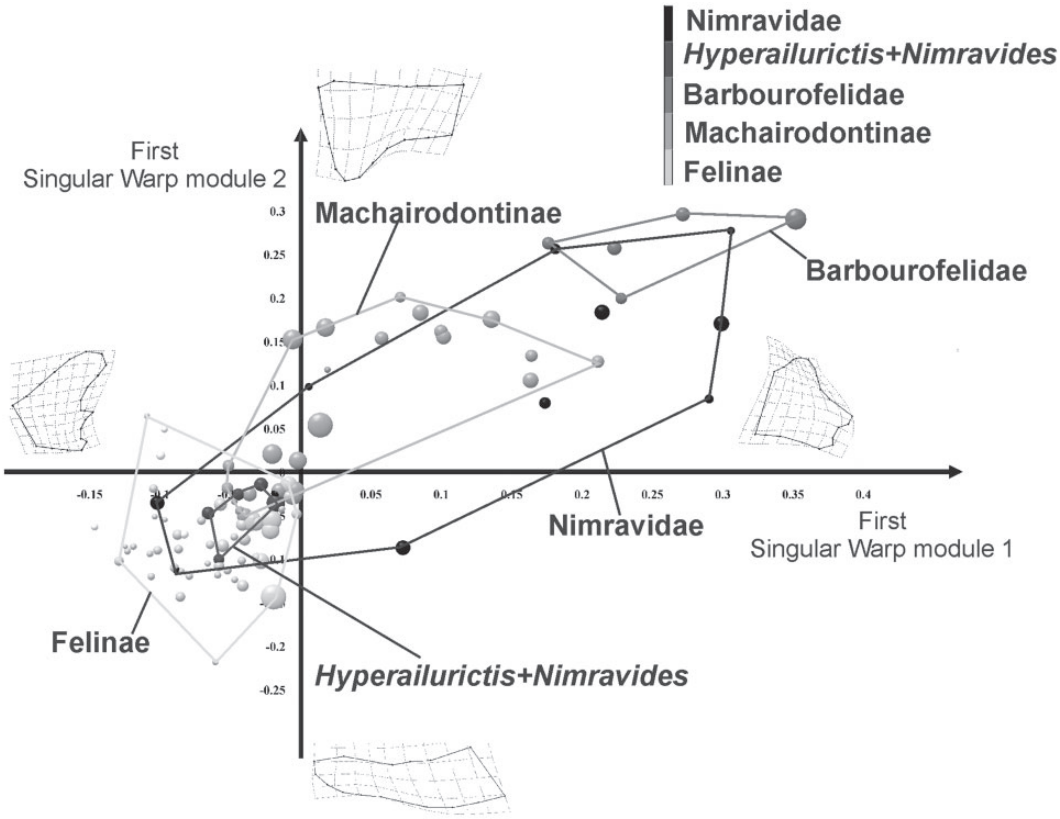

FIGURE 6. Morphological covariation between the two modules identified on the mandible according to PLS analysis performed on the pooled sample. Points dimension is proportional to species mean CS.

Linear Models and Comparative Methods

Table 3 reports results of phylogenetic ANOVA and MANOVA. As for stress variables, these procedures revealed that Barbourofelidae is the clade differing the most from the others. Size, on the other hand, does not seem significantly different among individual clades once phylogeny is accounted for. In the phylogenetic MANOVAs, only the Barbourofelidae–Felinae difference is significant. The Mantel test revealed the presence of phylogenetic signal in shape ($P < 0.001$). Using phylosig() function we found strong phylogenetic signal in both stress variables and CS ($P < 0.001$ for all the three variables).

Seven different evolutionary modes were tested (Table 4). As for surface traction, the best model in terms of AIC appears to be Ornstein–Uhlenbeck (OU with $\alpha = 0.07$). Yet, the analysis of Akaike weights reveals that the delta transformation proves to be a good alternative model. The fitted delta value (0.255) indicates a slowdown in the evolutionary rate of surface traction towards the recent. Both delta and OU models are statistically superior to Brownian motion (BM), as judged by likelihood ratio test (Table 4). The phylogenetic signal K in surface traction is 0.274, which is significantly different from 0 (i.e. no signal, $p = 0.002$). The evolution of von Mises stress is best described by lambda, and secondarily by OU model. Both these models proved statistically better than BM (Table 4). The phylogenetic signal in von Mises stress is small ($K = 0.300$) but significant ($P = 0.001$). Finally, the evolution of CS is best described by kappa, and secondarily by OU and lambda models, as assessed by Akaike weights (Table 4). The phylogenetic signal in CS is 0.241, which is significantly different from zero ($P = 0.002$).

Overall, the OU process is the best descriptor for surface traction and a good descriptor (albeit not the best) of von Mises stress and CS, indicating that there is a tendency to evolve towards an adaptive performance peak in cat-like carnivorans. The strength of selection of surface traction towards the peak (the fitted value alpha in OU) is very close to zero (which corresponds, virtually, to Brownian motion, Butler and King 2004). This is consistent with the finding that the phylogenetic signal is significant for the variables considered, as it is for CS (cf. Meloro and Raia 2010).

Table 5 shows multivariate regressions between shape data and stress variables. As for the whole mandible, this relationship is significant under PGLS. Using per-group size-free shape data (i.e. residuals of the per-clade regression between shape and size) we found smaller but still significant relationships under PGLS. This indicates that allometry is not responsible for the relationship between entire shape and stress variables.

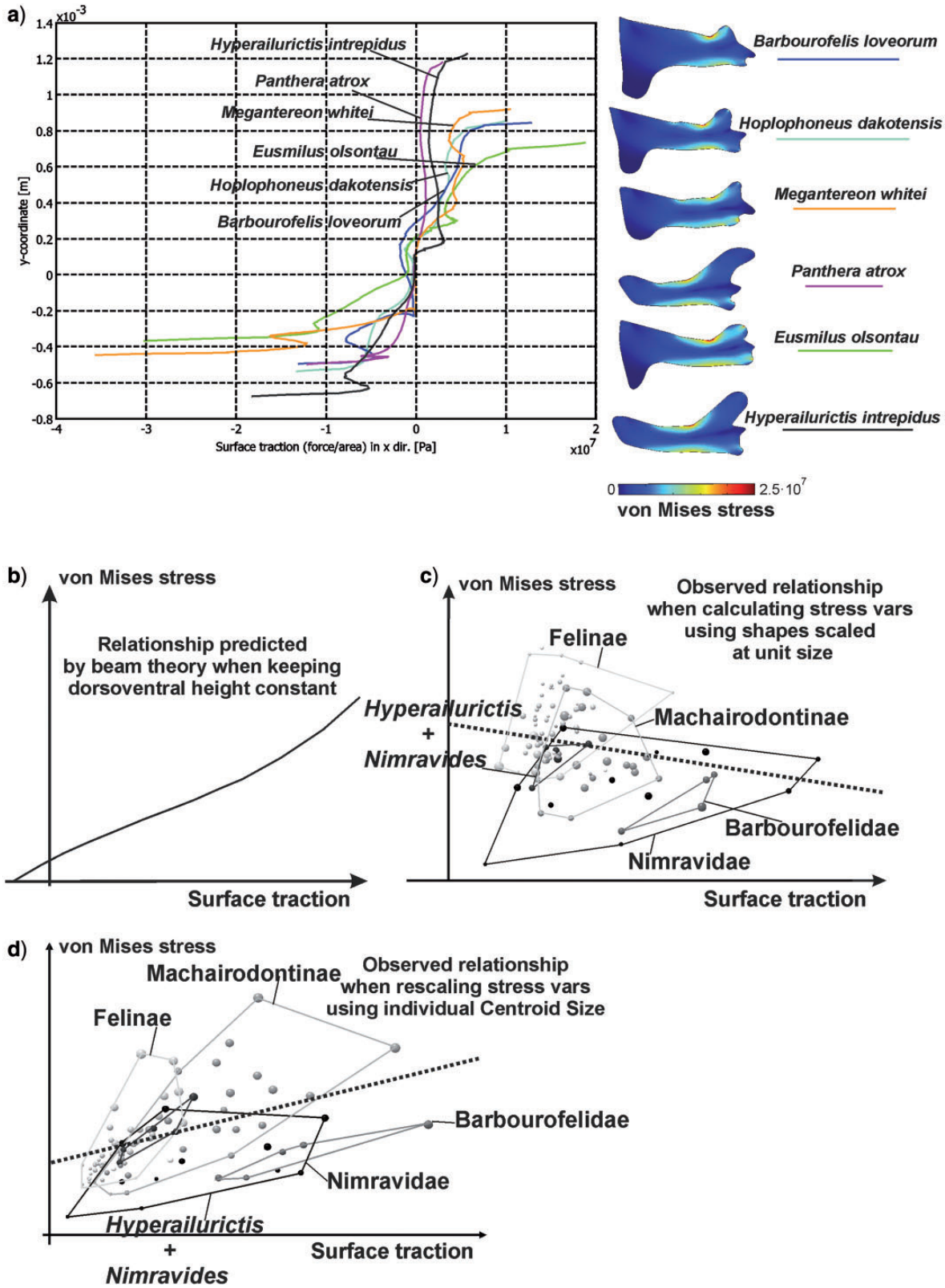

FIGURE 7. a) Surface traction plotted against y-coordinate of the boundary along which this variable has been measured. One typical representative of each family/subfamily is shown. b) Relationship predicted by beam theory when keeping dorsoventral height constant. c) Observed relationship between von Mises stress and surface traction. d) Observed relationship when both stress variables are re-multiplied by individual CS. Dotted line represents linear model interpolation.

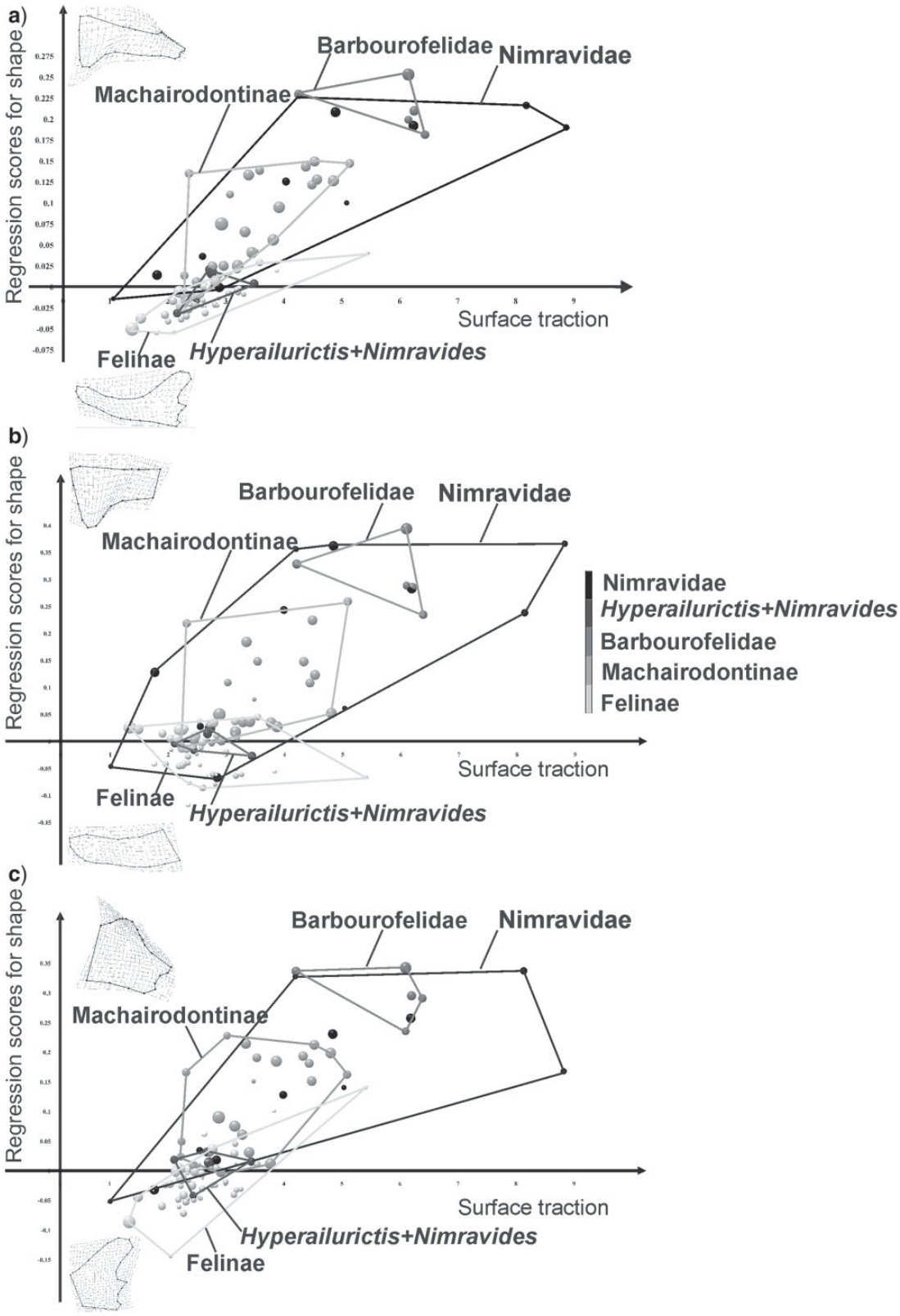

FIGURE 8. a) Relationship between entire mandible, b) mandibular corpus, and c) ascending ramus shapes and surface traction. Points dimension is proportional to species mean CS.

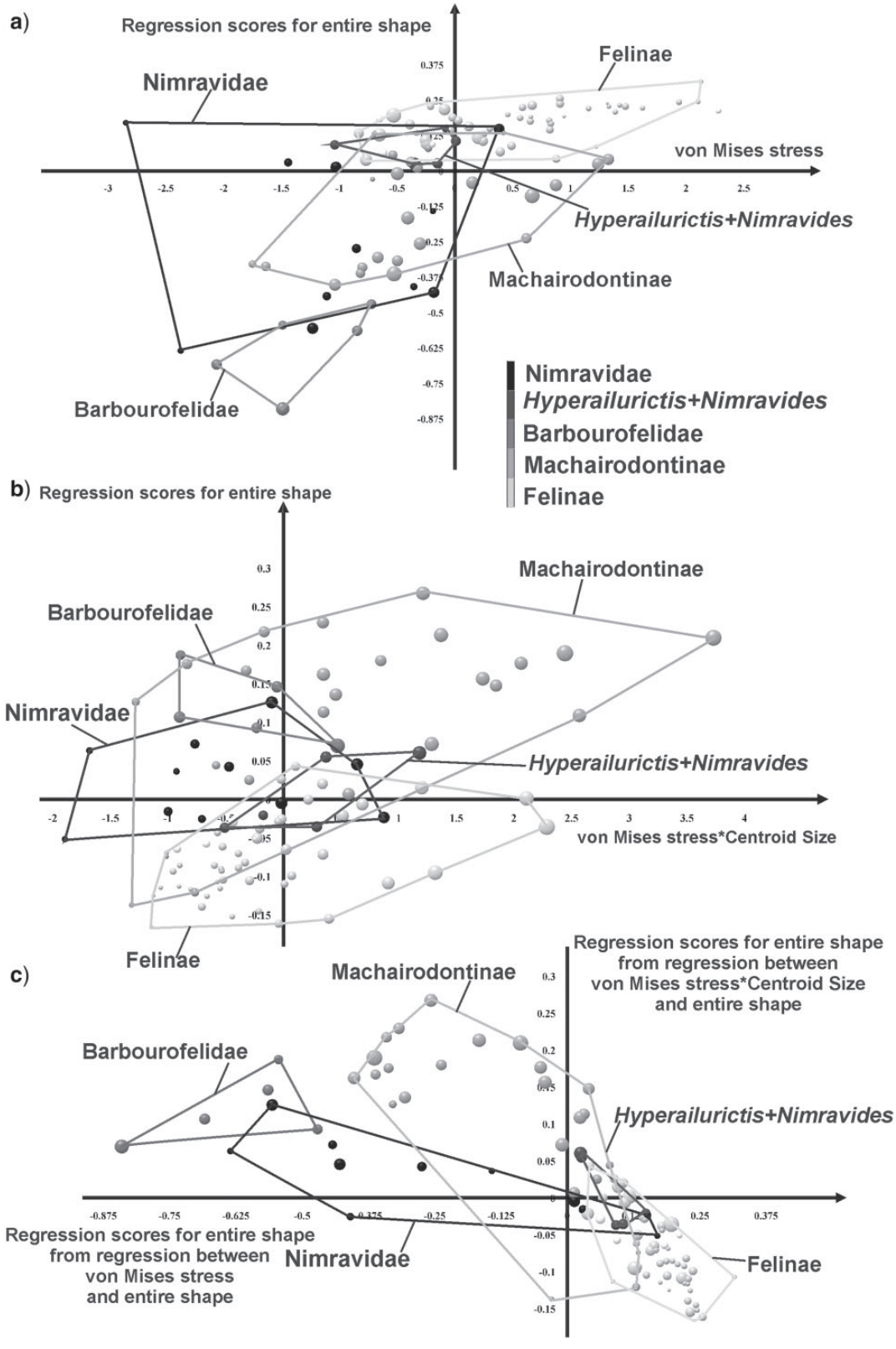

FIGURE 9. a) Regression between von Mises stress and shape; here Felinae appear as the most stressed. b) Regression between von Mises stress rescaled using original individual CS and shape. c) Regression scores for shape in a) versus regression scores for shape in b); they are negatively correlated.

TABLE 3. *P*-values of pairwise phylogenetic ANOVAs (on stress variables and size) and MANOVAs (on Shape data) between the five main clades under study

	Nimravidae	*Hyper.+Nimravides*	Barbourofelidae	Machairodontinae	Felinae
Phylogenetic ANOVA on surface traction					
Nimravidae	–	0.352	0.516	0.2837	**0.017**
Hyper.+Nimravides		–	**0.0010**	0.11	0.6783
Barbourofelidae			–	**0.0020**	**0.0010**
Machairodontonae				–	0.051
Felinae					–
Phylogenetic ANOVA on von Mises stress					
Nimravidae	–	0.39	0.74	0.21	0.055
Hyper.+Nimravides		–	**0.009**	0.90	0.060
Barbourofelidae			–	0.16	**0.005**
Machairodontonae				–	0.21
Felinae					–
Phylogenetic ANOVA on size					
Nimravidae	–	0.74	0.65	0.63	0.89
Hyper.+Nimravides		–	0.9191	0.80	0.57
Barbourofelidae			–	0.94	0.54
Machairodontonae				–	0.49
Felinae					–
Phylogenetic MANOVA on shape					
Nimravidae	–	0.9970	0.9850	0.9920	0.9191
Hyper.+Nimravides		–	0.4446	0.9710	0.8791
Barbourofelidae			–	0.9271	**0.0060**
Machairodontonae				–	0.6044
Felinae					–

Significant results are shown in bold.

TABLE 4. Model parameters for the phenotypes under study

Surface traction								
Model	Fitted parameter	Log-likelihood	LRT	AIC	AIC diff	Akaike weights	*K*	*P*-value ($K > 0$)
BM		−143.065		290.130	6.400	0.022		
lambda	0.984	−142.273	0.208	290.547	6.900	0.017		
delta	0.255	−139.153	0.005	284.307	0.610	0.390		
kappa	0.598	−141.371	0.066	288.743	5.100	0.041		
ou	0.075	−138.846	0.004	283.692	0.000	0.530	0.27	0.002
eb	0.000	−182.367	1.000	370.734	87.000	0.000		
white	–	−163.015	1.000	330.031	46.000	0.000		
von Mises stress								
BM		−127.057		258.114	5.600	0.030		
lambda	0.950	−123.270	0.006	252.541	0.000	0.486	0.30	0.001
delta	1.152	−126.980	0.694	259.959	7.400	0.012		
kappa	0.618	−125.005	0.043	256.009	3.500	0.084		
ou	0.068	−123.497	0.008	252.994	0.450	0.388		
eb	0.000	−179.736	1.000	365.471	113.000	0.000		
white	–	−146.704	1.000	297.407	45.000	0.000		
CS								
BM		87.751		−171.503	12.000	0.001		
lambda	0.875	93.258	0.001	−180.516	2.800	0.135		
delta	2.223	91.333	0.007	−176.666	6.700	0.019		
kappa	0.070	94.678	0.000	−183.356	0.000	0.546	0.24	0.001
ou	0.111	94.065	0.000	−182.130	1.200	0.299		
Eb	0.000	−173.335	1.000	352.669	536.000	0.000		
white	–	76.551	1.000	−149.102	34.000	0.000		

The best model found are shown in bold.

TABLE 5. PGLS models for shape-stress variables relationships

Procrustes coordinates	von Mises stress	Surface traction
PGLS		
Entire shape	$P = \mathbf{3.17e{-}15}$	$P = \mathbf{2.2e{-}16}$
Mandibular corpus	$P = \mathbf{2.2e{-}16}$	$P = \mathbf{0.0012}$
Ascending ramus	$P = \mathbf{1.97e{-}6}$	$P = \mathbf{2.2e{-}16}$
Size free shape data PGLS		
Entire shape	$P = \mathbf{2.85e{-}8}$	$P = \mathbf{2.2e{-}16}$
Mandibular corpus	$P = \mathbf{1.04e{-}9}$	$P = \mathbf{0.0002}$
Ascending ramus	$P = \mathbf{0.0017}$	$P = \mathbf{1.67e{-}12}$

Significant results are shown in bold.

All relationships were significant also for single modules under PGLS, even using size-free shape data.

Observed von Mises stress is negatively related to observed surface traction ($R^2 = 0.045$; Fig. 7c), contrary to what is predicted by beam theory (Fig. 7b), when keeping beam height constant. This relationship is significant under PGLS ($P = 0.0059$). Von Mises stress is negatively correlated with the area of mandibular corpus ($R^2 = 0.44$; PGLS $P = 3.5e{-}05$) and positively correlated (albeit weakly) with the area of ascending ramus ($R^2 = 0.048$; PGLS $P = 0.00013$). Conversely, surface traction is positively related to the area of mandibular corpus ($R^2 = 0.59$; PGLS $P = 2e{-}16$) and negatively to the area of ascending ramus ($R^2 = 0.53$; PGLS $P = 2.3e{-}08$). When von Mises stress and surface traction are re-multiplied by the original CSs their relationship becomes positive and significant under PGLS ($R^2 = 0.26$; PGLS $P = 1.8e{-}14$; Fig. 7d). This suggests that the negative relationship between von Mises stress and surface traction is due to allometric effects.

Table 6 shows results for linear-model regressions between clade *RV*s, per-clade averaged stress values, and per-clade averaged size values. Relationships between stress variables and *RV*s (Fig. 10) are always significant even using *RV*s calculated on size-free shape data, thus suggesting that intraclade allometry did not impact on this relationship. The relationships between per-clade averaged size values and clades *RV*s or stress variables are not significant, indicating no impact of interclade allometry. This could be read together with the results of PLS analysis and relationships between von Mises stress and mandibular modules areas. Our interpretation is that there is a strong association between the degree of morphological integration and the biomechanical performance due to a structural compensation of mandibular corpus in response to the dramatic morphological changes in the posterior part of the mandible of sabertoothed cats (see discussion below). Neither relationship between surface traction and size nor the relationship between von Mises stress and size is significant under PGLS. Together with results reported above, the negative relationship between von Mises stress and size explains why stress variables *scaled at unit size* show a pattern inverse to that predicted by beam theory. This is definitively a consequence of the covariation between the two submodules, and of the increase of mandibular corpus area (thus increasing the denominator of the mean von Mises stress) which is typical of the sabertooth mandible.

DISCUSSION

The combined use of GM and FEA provides a powerful methodological tool to interpret macroevolutionary transformation in mandible size, shape, and mechanical performance. We applied this ensemble of methods to study morphological variation in the mandible of cat-like carnivores.

In recent years several works focused on the craniofacial morphological variation in this group (Martin 1980; Van Valkenburgh 2007; Meloro et al. 2008, 2011 among others), and in cat-like species in particular (Samuels and Van Valkenburg 2009; Sakamoto et al. 2010; Slater and Van Valkenburgh 2008, 2009; Prevosti et al. 2010; Lencastre-Sicuro and Oliveira 2010; Meloro and Slater 2012). Most of these papers addressed the profound functional differences between modern cats and extinct sabertooths. This issue has been debated since the very first discoveries of sabertooths (Warren 1853; Riggs 1934; Simpson 1941)—a highly distinctive morphology that occurs independently multiple times in mammals (i.e. within Felidae, Barbourofelidae, Nimravidae, Creodonta, and even Marsupialia). Our results demonstrate that cat-like carnivorans evolved fairly conservative mandibular morphology within distinct clades (Meloro and Raia 2010). The regression between size and shape of the pooled sample suggests the presence of a strong evolutionary allometric signal in mandibular morphology. Felinae and Barbourofelidae are the clades showing the strongest allometric effects, whereas no allometric effects are apparent in nimravid mandibles. This result confirms recent findings by Slater and Van Valkenburgh (2009) and Meloro and Slater (2012).

Allometry significantly impacts Felinae because high body size variation in this group probably represented the most "rapid" way of differentiating niches within a young and morphologically very homogeneous group such as true cats. This agrees with previous findings about the evolutionary tempo and mode of carnassial size evolution in Carnivora as a whole (Meloro and Raia 2010). Sabertooths are less variable in body size than other felines, and are generally large. Ecomorphological differentiation among sabertooths took place through the relative elongation of the upper canines and includes two distinct morphotypes: the saber- and the dirk-toothed cats. Meloro and Slater (2012) recently highlighted that relative canine length has a strong influence on morphological integration of the skull in long-canine cats. This likely is the case for the mandible as well. We found that morphological integration was strongest in Barbourofelidae, which is the most "extreme" dirk-toothed clade.

One of the most interesting results of this study is the significant relationship between functional integration and stress data. In the particular context of our study, this relationship indicates that the dramatic temporo-mandibular modifications of the sabertoothed morphology required a strengthening of functional covariation between mandible submodules. We found mandibles were more stressed in sabertooths, mainly in the ascending ramus, than in modern felids (in keeping with McHenry et al. 2007) under the same scale (unit size) and loading conditions. This happens because of the strong covariation of the mandibular corpus with the posterior part of the mandible implies strong dorsoventral buttressing in sabertooths. Natural selection is expected to mould shapes according to functional demands. The more demanding is the function, the more tightly body structures involved in the function must be integrated. Modularity and integration are flip sides of the same coin. They involve the organization of whole structures in partially independent morpho-genetic and functional modules (Klingenberg 2009, 2010, rephrased). As rigid solids, bones are subjected to physical forces. So variation in shape produces variation in bone's ability to achieve a particular mechanical function in response to external stresses. This variation is constrained by the mechanical limits of the bone material. The fact that the OU model describes well the evolution of surface traction shows that species tend to converge towards optimal stress values. In our view, the tight link between integration and stress loadings evolved to overcome such a constraint. Sabertooths, for example, had to gape their mouth wide, in order to use the long canines (Christiansen 2011). This is ubiquitous among sabertooths, and comes at the cost of higher stress in the ascending ramus (McHenry et al. 2007, this study). This cost is partly counteracted by improving the morphological integration of the mandible as a whole.

Few works related morphological integration and function (Young and Badayev 2006; Klingenberg 2010; Monteiro and Nogueira 2010; Piras et al. 2010; Klingenberg 2010 for a review). As meaningfully synthesized by Klingenberg et al. (2010), functional modules are those parts that perform specific functions irrespectively of morphogenetic (developmental) modular organization. Functional and developmental integration could or could not coincide. On the basis of different works carried out at different taxonomic levels, it seems that their concordance may be dependent on the evolutionary scale of observation. In fact, investigation of integration (functional and developmental; Klingenberg et al. 2010) within single species has shown that developmental modules do not match functional modules. Conversely, within genus (between species) analyses (Young and Badayev 2006) show a strong concordance between developmental and functional modules. Monteiro and Nogueira (2010), in studying phyllostomid bats, found that functional integration is decoupled from developmental integration in specialized, but not in generalist species.

Our study belongs to the main stream of research in this field. Yet, it differs from previous studies for a number of reasons: first, we compared species and genera belonging to different families within a large and ancient clade, thus greatly increasing the taxonomic scale of investigation; second, we included extinct species even at the base of our phylogeny thus increasing the temporal scale of observation; third, we did not compare functional and morphogenetic modules, thereby testing if they concide, but rather we compared an a priori defined functional organization between clades; finally, we quantitatively defined function in term of structural stress.

We suggest that the importance of constraints imposed by genetic expression, natural selection and shared ancestry on modular organization varies according to taxonomic and temporal scales of observation. Patterns of developmental integration within individuals (or species, at the best) can be determined by relatively environment-independent selection for developmental homeostasis, whereas patterns among species (and even more so for genera and families) reveal the relative importance of current selection regimes, thus making integration more readily investigated in terms of functional demands. A future challenge could be testing if the functional modular organization we explored here coincides with developmental modularity. It would be desirable to test this at the same observational

TABLE 6. Relationships between morphological integration, per-clade averaged stress variables and per-clade averaged size values

Using *RV*s calculated on original shape variables			
	β, R^2, permutation P−value	β, R^2, permutation P−value	β, R^2, permutation P−value
	von Mises stress	Surface traction	Per clade averaged size values
*RV*s	**−2.4*e*−7; 0.94; 0.02**	**1.39*e*−7; 0.81; 0.03**	0.02; 0.37; 0.29
Per clade averaged size values	9.6e5; 0.11; 0.6	−7.9e5; 0.19; 0.4	
	β, R^2, permutation P−value	β, R^2, permutation P−value	β, R^2, permutation P−value
Using *RV*s calculated on size free shape variables			
*RV*s	**−2.15*e*−7; 0.95; 0.008**	**1.51*e*−7; 0.90; 0.03**	0.018; 0.16; 0.52

Significant results are shown in bold.

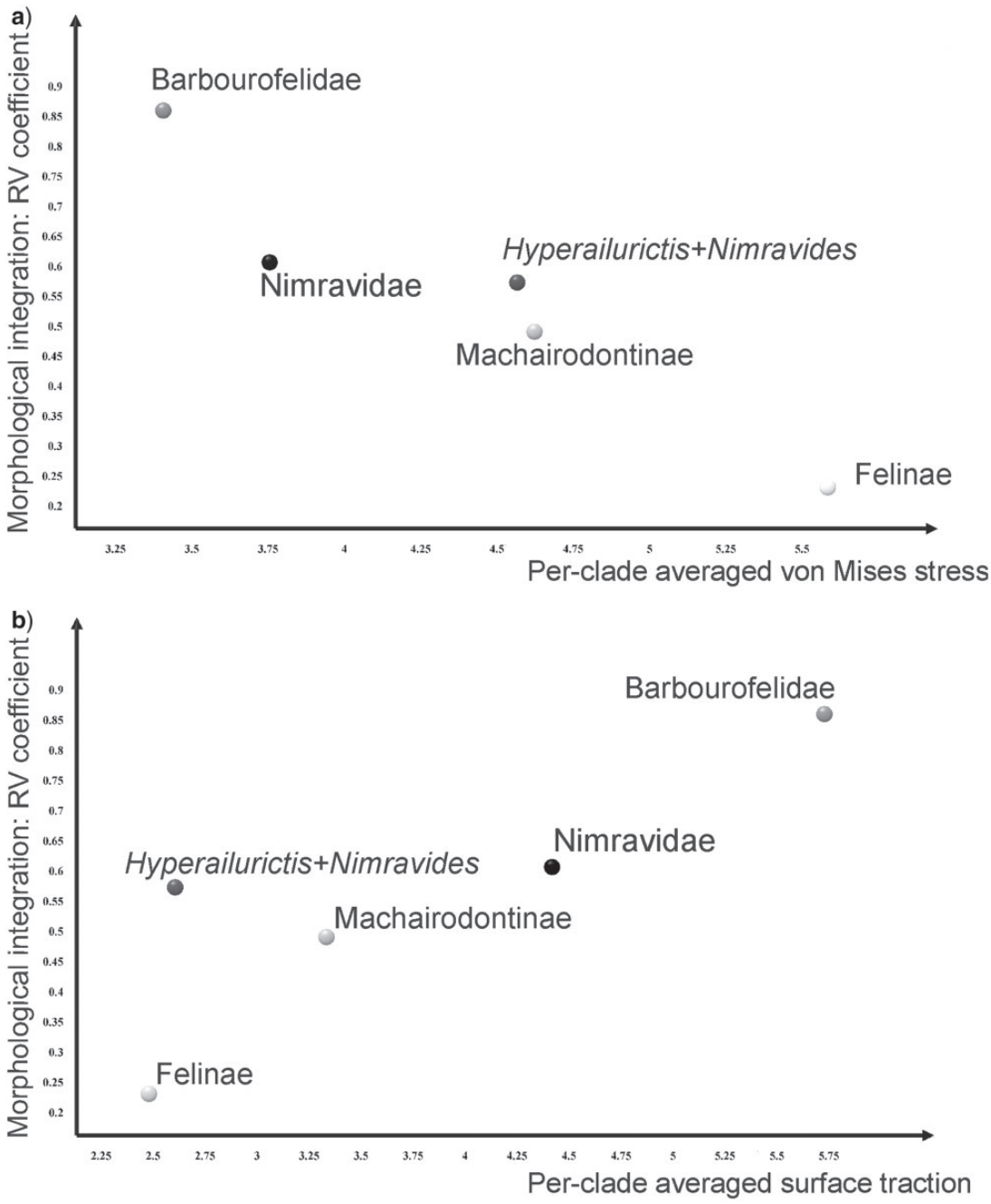

FIGURE 10. Relationships between per-clade averaged stress variables and *RV* coefficients.

(taxonomic-phylogenetic) scale of our study. Ecological factors and the selection gradients on the fitness landscape of the adaptive radiation are important for understanding the evolutionary integration of complex morphological structures (Monteiro and Nogueira 2010).

A result apparently in contradiction with previous studies deserves special attention: at unit sizes von Mises stress of the whole mandible diminishes in sabertoothed species because of the increase in dorsoventral buttressing of the mandibular corpus, whereas it is much less related to the area of posterior part. That causes the observed relationship between von Mises stress and surface traction in Figure 7c. This must be contextualized in the "equal scaling" strategy under which we calculated our stress variables. In fact, our results regarding structural performance seem to alternatively agree (as for surface traction) or disagree (as for von Mises stress) to those obtained by McHenry et al. (2007). McHenry et al. (2007) compared one specimen of *Panthera leo* to one specimen of *Smilodon fatalis*. They applied a sophisticated 3D FEA simulation to a mandible with an articulated skull. They also estimated

bite forces for the two species and found that *S. fatalis* had smaller bite force, higher von Mises stress and smaller structural resistance as compared with *P. leo*. There are significant differences between the present study and that of McHenry et al. McHenry et al. (2007) used a 3D model of both skull and mandible and they did not scale shapes at common size (as in our simulations). The lion in our sample presents a larger mandibular CS than *Smilodon*. Still, they did not assess statistically the structural behaviour of a large cat-like sample species and simulated muscle insertions and contractions rather than imposing a constant bite force. Here, we specifically wanted to compare several shapes at a common size and under equal loadings. Our surface traction results indicate just what McHenry et al. (2007) stated about the concentration of a large component of the stress in correspondence to the coronoid process: sabertoothed species show a surface traction that is larger than in conical forms. This is clearly illustrated in Fig. 8a that, structurally, suggests a pattern similar to what McHenry et al. (2007) found. By contrast, we contend that, *at equal scale*, mean von Mises stress diminishes in sabertooths because of the mandible-enlarged anterior area (the buttressing), which increases the denominator in mean von Mises integration. This enlargement is clearly visible in Fig. 5c and in Fig. 6 showing the covariation between the two modules. When von Mises stress is re-scaled using the original CSs, even this variable agrees the general suggestion of McHenry et al. (2007) that sabertoohed mandibles had to withstand higher stress loads (Fig. 7d).

3D models are reliable in terms of validative power of results and of inner morphology and material properties. However, it is impossible to apply this methodology to the data set we presented here.

A final argument regarding mandible abduction should be addressed. Christiansen (2011), studying 14 species of extinct and extant felids, pointed out that sabertooths could open their mouth at particularly large angles. This implies a rearrangement of both muscle insertions on the mandible and of the global shape of the cranium itself. During the bite a sabertooth had to fill the difference in gape angle with a conical-toothed species by progressively closing its jaws. As the bite started, the orthogonal component of bite force was smaller in sabertooths due to the large gape angle. However, the angle between the temporomandibular joint and the theoretical force output is always larger in derived sabercats than in extant felids at *any* gape angle over occlusion. This is due to the covarying geometric arrangement of mandible and skull (Christiansen 2011, figure 2). In fact, it was very likely that jaw abduction starting from extreme gape angles was achieved by head depression rather than by the force of jaw adductors. We integrated these results with those related to the higher morphological integration in derived sabertoothed species in comparison with nonsabertoothed forms. This, rather than an adaptation to higher bite force, could be interpreted as a response to the stress affecting the mandible (as explained above) caused by a higher surface traction along the mandible posterior margin. In fact, under static conditions, the surface traction increases because of the reduction in the height of the coronoid process. This is counteracted by the posterior shifting of the mandibular condyle that increases the inlever moment arm for the temporalis muscle, as pointed out by Bryant and Russell (1995) and Christiansen (2011).

Possible refinement of our study could come from dynamic simulations and from expanding our data set to complete skulls, in order to study the covariation between mandible and skull. However, for many species of our data set the skull is not known. Moreover, as stated in Online Appendix II (available from Dryad data repository; doi:10.5061/dryad.kp8t3), significant changes in the phylogeny (but presumably not small changes deep in the topology) could change the results of our PGLS analyses.

Supplementary Material

Supplementary material, inlcuding online-only appendices, is available at http://datadryad.org in the Dryad data repository: doi:10.5061/dryad.kp8t3.

Funding

Carlo Meloro museum visits were supported by the European Community's program 'Structuring the European Research Area' under Synthesys at the Museo Nacional de Ciencias Naturales (ES-TAF 858), Muséum National d'Histoire Naturelle (FR-TAF 1680) for the project 'The evolution of feeding habits in extinct European carnivores' while the visit at the Royal Museum for Central Africa was supported by the project 'Ecomorphology of extant African carnivores' (BE-TAF 4901).

Acknowledgments

We are grateful to many museum institutions and members of staff for allowing us access to the collection in their care. The Governments of Kenya and Tanzania kindly provided permission to Carlo Meloro to study fossil collection at the Kenya National Museum (Nairobi) supported by the Leverhulme Trust project "Taxon-Free Palaeontological Methods for Reconstructing Environmental Change" (F/00 754/C). We also thank Stefano Gabriele, Valerio Varano, and Gabriele Sansalone for useful discussions during manuscript preparation. We are grateful to Ronald DeBry, Frank (Andy) Anderson, Norm MacLeod, and three anonymous reviewers for the kind and insightful review of this manuscript.

References

Adams D.C., Rohlf F.J., Slice D.E. 2004. Geometric morphometrics: ten years of progress following the 'revolution'. Ital. J. Zool. 71:5–16.

Andersson K., Werdelin L. 2005. Carnivora from the Late Miocene of Lantian, China. Vert. Pal. 43(4):256–271.
Andersson K., Norman D., Werdelin L. 2011. Sabretoothed carnivores and the killing of large prey. PlosOne. 6:e24971.
Atchley W.R. 1993. Genetic and developmental aspects of variability in the mammalian mandible. In: Hanken J., Hall B.K., editors. The skull, vol. 1: development. Chicago: University of Chicago Press. p. 207–247.
Atchley W.R., Hall B.K. 1991. A model for development and evolution of complex morphological structures. Biol. Rev. Cambr. Phil. Soc. 66:101–157.
Atchley W.R., Nordheim E.V., Gunsett F.C., Crump P.L. 1982. Geometric and probabilistic aspects of statistical distance functions. Syst. Zool. 31:445–460.
Beaumont G. de. 1990. Contribution a l'étude du genre *Nimravides* KITTS (Mammalia, Carnivora, Felidae). L'espéce *N. pedionomus* (MACDONALD). Arch. Sci. Genéve. 43:125–157.
Badyaev A.V., Foresman K.R. 2000. Extreme environmental change and evolution: stress-induced morphological variation is strongly concordant with patterns of evolutionary divergence in shrew mandibles. Proc. R. Soc. B. Biol. Sci. 267:371–377.
Badyaev A.V., Foresman K.R. 2004. Evolution of morphological integration. I. Functional units channel stress–induced variation in shrew mandibles. Amer. Nat. 163(6):868–879.
Badyaev A.V., Foresman K.R., Young R.L. 2005. Evolution of morphological integration. II. Developmental accommodation of stress-induced variation in shrew mandibles. Am. Nat.166:382–395.
Blankers T., Adams D.C., Wiens J.J. 2012. Ecological radiation with limited morphological diversification in salamanders. J Evol Biol 25: 634–646.
Blomberg S.P., Garland Jr. T., Ives A.. 2003. Testing for phylogenetic signal in comparative data: behavioral traits are more labile. Evolution 57(4):717–745.
Bookstein F.L. 1986. Size and shape spaces for landmark data in two dimensions. Stat. Sci. 1:181–242.
Bookstein F.L. 1991. Morphometric tools for landmark data: geometry and biology. Cambridge: Cambridge University Press.
Bookstein F.L.1997, Landmark methods for forms without landmarks: morphometrics of group differences in outline shape. Med. Image. Anal. 1:225–243.
Bookstein F.L., Streissguth A.P., Sampson P.D., Connor P.D., Barr H.H. 2002. Corpus callosum shape and neuropsychological deficits in adult males with heavy fetal alcohol exposure. NeuroImage. 15:233–251.
Bryant H.N., Russell A.P. 1995. Carnassial functioning in nimravid and felid sabertooths: theoretical basis and robustness of inferences. In: Thomason J.J., editor. Functional morphology in vertebrate paleontology, Cambridge University Press. p. 116–135.
Cardini A., Tongiorgi P. 2003. Yellow-bellied marmots (*Marmota flaviventris*) 'in the shape space' (Rodentia, Sciuridae): sexual dimorphism, growth and allometry of the mandible. Zoomorphology. 122:11–23.
Cheverud J.M. 2004. Modular pleiotropic effects of quantitative trait loci on morphological traits. In: Schlosser G., Wagner G.P., editors. Modularity in development and evolution. Chicago: University of Chicago Press. p. 132–153.
Cheverud J.M., Hartman S.E., Richtsmeier J.T., Atchley W.R. 1991. A quantitative genetic analysis of localized morphology in mandibles of inbred mice using finite element scaling analysis. J. Craniofac. Genet. Dev. Biol. 11:122–137.
Cheverud J.M., Leamy L.J., Routman E.J. 1997. Pleiotropic effects of individual gene loci on mandibular morphology. Evolution. 51:2004–2014.
Cheverud J.M., Ehrich T.H., Vaughn T.T., Koreishi S.F., Linsey R.B., Pletscher L.S. 2004. Pleiotropic effects on mandibular morphology II: differential epistasis and genetic variation in morphological integration. J. Exp. Zool. B: Molec. Develop. Evol. 302B:424–435.
Christiansen P. 2008. Evolution of skull and mandible shape in cats (Carnivora: Felidae). PlosOne. 3:e2807.
Christiansen P. 2011. A dynamic model for the evolution of sabrecat predatory bite mechanics. Zool. J. Linn. Soc. 162:220–242.
Claude J. 2008. Morphometrics with R. New York: Springer.
Crusafont-Pairó M., Truyols-Santonja J. 1956. A biometric study of evolution of fissiped carnivores. Evolution. 10:314–332.
Crusafont-Pairó M., Truyols-Santonja J. 1957. Estudios masterométricos en la evolución Fisípedos. I. Los módulos angulares a y b. II. Los parámetros lineales P, C, y T. Bol. Inst. Geol. Min. España. 68:1–140.
Crusafont-Pairó M., Truyols-Santonja J. 1958. A quantitative study of stasigenesis in fissipede carnivores. Nature. 181:289–290.
Dray S., Dufour, A.B. 2007. The ade4 package: implementing the duality diagram for ecologists. J. Stat. Soft. 22: 1–20.
Dumont E.R., Grosse I.R., Slater G. 2009. Requirements for comparing the performance of finite element models of biological structures. J. Theoret. Biol. 256:96–103.
Ehrich T.H., Vaughn T.T., Koreishi S.F., Linsey R.B., Pletscher L.S., Cheverud J.M. 2003. Pleiotropic effects on mandibular morphology II. Developmental morphological integration and differential dominance. J. Exp. Zool. B: Molec. Develop. Evol. 296B:58–79.
Escoufier Y. 1973. Le traitement des variables vectorielles. Biometrics. 29:751–760.
Ewer R.F. 1973. The carnivores. Cornell University Press, New York.
Farke A.A. 2008. Frontal sinuses and head-butting in goats: a finite element analysis. J. Exp. Biol. 211:3085–3094.
Felsenstein J. 1985. Phylogenies and the comparative method. Am. Nat. 125:1–15.
Feranec R.S. 2008. Growth differences in the saber-tooth of three felid species. Palaios. 23:566–569.
Figueirido B., Serrano-Alarcón F. J., Slater G. J., Palmqvist P.. 2010. Shape at the cross-roads: homoplasy and history in the evolution of the carnivoran skull towards herbivory. Journal of Evol. Biol. 23: 2579–2594.
Figueirido B., MacLeod N., Krieger J., De Renzi M., Pérez-Claros J.A., Palmqvist P. 2011. Constraint and adaptation in the evolution of carnivoran skull shape. Paleobiology 37: 490–518.
Garland T.Jr. 1992. Rate tests for phenotypic evolution using phylogenetically independent contrasts. Am. Nat. 140:509–519.
Garland T.Jr., Bennett A.F., Rezende E.L. 2005. Phylogenetic approaches in comparative physiology. J. Exp. Biol. 208:3015–3035.
Geraads D., Güleç E. 1997. Relationships of *Barbourofelis piveteaui* (OZANSOY, 1965), a Late Miocene nimravid (Carnivora, Mammalia) from Central Turkey. J. Vert. Pal. 17(2):370–375.
Goodall C. 1991. Procrustes methods in the statistical analysis of shape. J. R. Statist. Soc. B. 53:285–339.
Gröning F., Liu J., Fagan M.J., O'Higgins P. 2009. Validating a voxel-based finite element model of a human mandible using digital speckle pattern interferometry. J. Biomech. 42:1224–1229.
Harmon L.J., Weir J., Brock C, Glor R.E., Challenger W. 2008. GEIGER: investigating evolutionary radiations. Bioinformatics 24:129–131.
Herring S.W. 1980. The ontogeny of mammalian mastication. Amer. Zool. 25(2):339–350.
Herring S.W. 1993. Functional Morphology of Mammalian Mastication. Amer. Zool. 33(3):289–299.
Holliday J.A., Steppan S.J. 2004. Evolution of hypercarnivory: the effect of specialization on morphological and taxonomic diversity. Paleobiology. 30:108–128.
Johnson W.E., Eizirik E., Pecon-Slatter J., Murphy W.J., Antunes A., Teeling E., O'Brien S.J. 2006. The late Miocene radiation of modern Felidae: a genetic assessment. Science. 311:73–77.
Klingenberg C. P. 2009. Morphometric integration and modularity in configurations of landmarks: Tools for evaluating a-priori hypotheses. Evol. Dev. 11:405–421.
Klingenberg C. P. 2010. Evolution and development of shape: integrating quantitative approaches. Nat. Rev. Gen. 11:623–635.
Klingenberg C.P., Barluenga M., Meye A. 2003. Body shape variation in cichlid fishes of the *Amphilophus citrinellus* species complex. Biol. J. Linn. Soc. 80:397–408.
Klingenberg C.P., V. Debat, Roff D.A. 2010. Quantitative genetics of shape in cricket wings: developmental integration in a functional structure. Evolution. 64:2935–2951.
Klingenberg C.P., Leamy L.J. 2001. Quantitative genetics of geometric shape in the mouse mandible.Evolution. 55:2342–2352.
Klingenberg C.P., Leamy L.J., Cheverud J.M. 2004. Integration and modularity of quantitative trait locus effects on geometric shape in the mouse mandible. Genetics. 166:1909–1921.

Klingenberg C.P., Leamy L.J., Routman E.J., Cheverud J.M. 2001. Genetic architecture of mandible shape in mice: effects of quantitative trait loci analyzed by geometric morphometrics. Genetics. 157: 785–802.
Kupczik K., Dobson C.A., Fagan M.J., Crompton R.H., Oxnard C.E., O'Higgins P. 2007. Assessing mechanical function of the zygomatic region in macaques: validation and sensitivity testing of finite element models. J. Anat. 210:41–53.
Kurtén B., Anderson E. 1980. Pleistocene mammals of North America. New York: Columbia University Press.
Leamy L.J., Routman E.J., Cheverud J.M. 2002. An epistatic genetic basis for fluctuating asymmetry of mandible size in mice. Evolution. 56:642–653.
Lencastre-Sicuro F., Oliveira L.F.B. 2010. Skull morphology and functionality of extant Felidae (Mammalia: Carnivora): a phylogenetic and evolutionary perspective. Zool. J. Linn. Soc. 161:414–462.
MacLeod N. 1999, Generalizing and extending the eigenshape method of shape visualization and analysis. Paleobiology 25:107–138.
Maddison W..P, Maddison D.R. 2010. Mesquite: A modular system for evolutionary analysis. Version 2.73.
Márquez E.J. 2008. A statistical framework for testing modularity in multidimensional data. Evolution. 62:2688–2708.
Martin L.D. 1980. Functional morphology and the evolution of cats. Trans. Nebr. Acad. Sci. 8:141–154.
Martin L.D., Babiarz J.P., Naples V.L., Hearst J. 2000. Three ways to be a saber-toothed cat. Naturwissenschaften. 87:41–44.
McHenry C.R., Wroe S., Clausen P.D., Moreno K., Cunningham E. 2007. Supermodeled sabercat, predatory behavior in *Smilodon fatalis* revealed by high-resolution 3D computer simulation. Proc. Nat. Acad. Sci. 104:16010–16015.
Meachen-Samuels, J. A. 2012. Morphological convergence of the prey-killing arsenal of sabertooth predators. Paleobiology 38:1–14.
Meloro C. 2011. Feeding habits of Plio-Pleistocene large carnivores as revealed by the mandibular geometry. J. Vert. Pal. 31:428–446.
Meloro C., Raia P. 2010. Cats and dogs down the tree: the tempo and mode of evolution in the lower carnassial of fossil and living carnivore. Evol. Biol. 37:177–186.
Meloro C., O'Higgins P. 2011. Ecological Adaptations of mandibular form in fissiped carnivore. J. Mammal. Evol. 18:185–200.
Meloro C., Slater G.J. 2012. Covariation in the skull modules of cats: the challenge of growing saber-like canines. J. Vert. Pal. 32: 677–685.
Meloro C., Raia P., Piras P., Barbera C., O'Higgins P. 2008. The shape of the mandibular corpus in large fissiped carnivores: allometry, function and phylogeny. Zool. J. Linn. Soc. 154:832–845.
Meloro C., Raia P., Carotenuto F., Cobb S.N. 2011. Phylogenetic signal, function and integration in the subunits of the carnivoran mandible. Evol. Biol. 38:465–475.
Mevik B.H., Wehrens R. 2007. The pls Package: Principal Component and Partial Least Squares Regression in R; J. Stat.Soft. 18:1–24.
Monteiro L.R., Nogueira M.R. 2010. Adaptive radiations, ecological specialization, and the evolutionary integration of complex morphological structures. Evolution 64:724–744.
Morlo M., Peigné S., Nagel D. 2004. A new species of *Prosansanosmilus*: implications for the systematic relationships of the family Barbourofelidae new rank (Carnivora, Mammalia). Zool. J. Linn. Soc. 140:43–61.
Mullin, S.K., Taylor, P.J. 2002. The effects of parallax on geometric morphometric data. Comp. Biol. Med. 32:455–464.
Peigné S. 2003. Systematic review of European Nimravinae (Mammalia, Carnivora, Nimravidae) and the phylogenetic relationships of Palaeogene Nimravidae. Zool. Scripta. 32(3):199–229.
Perez S.I., Bernal V., Gonzalez P.N. 2006. Differences between sliding semi-landmark methods in geometric morphometrics, with an application to human craniofacial and dental variation. J. Anat. 208:769–784.
Pierce S.E., Angielczyk K.D., Rayfield E.J. 2008. Patterns of morphospace occupation and mechanical performance in extant crocodilian skulls: a combined geometric morphometric and finite element modelling approach. J. Morphol. 269:840–864.
Pierce S.E., Angielczyk K.D., Rayfield E.J. 2009a. Shape and mechanics in thalattosuchian (Crocodylomorpha) skulls: implications for feeding behaviour and niche partitioning. J. Anat. 215:555–576.
Pierce S.E., Angielczyk K.D., Rayfield E.J. 2009b. Morphospace occupation in thalattosuchian crocodylomorphs: skull shape variation, species delineation, and temporal patterns. Palaeontology. 52:1057–1097.
Piras P., Maiorino L., Raia P., Marcolini F., Salvi D., Vignoli L., Kotsakis T. 2010. Functional and phylogenetic constraints in Rhinocerotinae craniodental morphology. Evol. Ecol. Res.12:897–928.
Piras P., Marcolini F., Claude J., Ventura J., Kotsakis T., Cubo J. 2012a. Ecological and functional correlates of molar shape variation in European populations of *Arvicola* (Arvicolinae, Rodentia). Zool. Anz. 251:335–343.
Piras P., Sansalone G., Teresi L., Kotsakis T., Colangelo P., Loy, A. 2012b. Testing convergent and parallel adaptations of talpids humeral mechanical performance by means of Geometric Morphometrics and Finite Element Analysis. J. Morph. 273:696–711.
Polly P.D. 2005. Development and phenotypic correlations: the evolution of tooth shape in *Sorex araneus*. Evol. Develop. 7:29–41.
Prevosti F.J., Turazzini G.F., Chemisquy M.A. 2010. Morfología craneana en tigres dientes de sable: alometría, función y filogenia. Ameghiniana 47:239–256.
Raia P., Carotenuto F., Meloro C., Piras P., Pushkina D. 2010. The shape of contention. adaptation, history and contingency in ungulate mandibles. Evolution. 64:1489–1503.
Rayfield E.J. 2007. Finite element analysis and understanding the biomechanics and evolution of living and fossil organisms. Annu. Rev. Earth Planet. Sci. 35:541–576.
Rayfield E.J. 2011. Strain in the ostrich mandible during simulated pecking and validation of specimen-specific finite element models. J. Anat. 218:47–58.
Rayfield E.J., Norman D.B., Horner C.C., Horner J.R., May Smith P., Thomason J.J., Upchurch P. 2001. Cranial design and function in a large theropod dinosaur. Nature. 409:1033–37.
Revell L. J. 2010. Phylogenetic signal and linear regression on species data. Methods Ecol. Evol. 1:319–329.
Revell L. J. 2012, phytools: an R package for phylogenetic comparative biology (and other things). Meth. Ecol. Evol. 3:217–223.
Richmond B.G., Wright B.W., Grosse I., Dechow P.C., Ross C.F., Spencer M.A., Strait D.S. 2005. Finite element analysis in functional morphology. Anat. Rec. A Discov. Mol. Cell. Evol. Biol. 283:259–274.
Riggs E.S. 1934. A new marsupial saber-tooth from the Pliocene of Argentina and its relationships to other South American predacious marsupials. Trans. Amer. Phil. Soc. 24(1):1–32.
Rohlf F.J. 2001. Comparative methods for the analysis of continuous variables: geometric interpretations. Evolution. 55:2143–2160.
Rohlf F.J. 2006. A comment on phylogenetic corrections. Evolution. 60:1509–1515.
Rohlf F.J. 2010a. tpsDig, Digitize Landmarks and Outlines. Version 2.16. Department of Ecology and Evolution, State University of New York at Stony Brook.
Rohlf F.J., Slice D. E. 1990. Extensions of the procrustes method for the optimal superimposition of landmarks. Syst. Biol. 39:40–59.
Rohlf F.J, Corti, M. 2000. Use of two-block partial leastsquares to study covariation in shape. Syst. Biol. 49:740–753.
Ross C.F., Patel B.A., Slice D.E., Strait D.S., Dechow P.C., Richmond B.C., Spencer M.A. 2005. Modeling masticatory muscle force in finite element analysis: sensitivity analysis using principal coordinates analysis. Anat. Rec. 283A:288–299.
Rothwell T. 2003. Phylogenetic systematics of North American *Pseudaelurus* (Carnivora: Felidae). Am. Mus. Nov. 3403:1–64.
Sakamoto M., Lloyd G.T., Benton M.J. 2010. Phylogenetically structured variance in felid bite force: the role of phylogeny in the evolution of biting performance. J. Evol. Biol. 23:463–478.
Schlager S. 2013. Morpho: Calculations and visualizations related to Geometric Morphometrics. R package version 0.23.3. http://CRAN.R-project.org/package=Morpho
Samuels J.M., Van Valkenburg B. 2009. Craniodental indicators of prey size preference in the Felidae. Biol. J. Linn. Soc. 96:784–799.
Simpson G.G. 1941. The function of saber-like canines in carnivorous mammals. Am. Mus. Novit. 1130:1– 12.

Slater G.J., Van Valkenburgh B. 2008. Long in the tooth: evolution of sabertooth cat cranial shape. Paleobiology. 34(3):403–419.
Slater G. J., Van Valkenburgh B. 2009. Allometry and performance: the evolution of skull form and function in felids. J. Evol. Biol. 22:2278–2287.
Slater G. J., Dumont, E. R., Van Valkenburgh, B. 2009. Implications of predatory specialization for cranial form and function in canids. J. Zool. Lond. 278: 181–188.
Stayton C.T. 2009. Application of thin-plate spline transformations to finite element models, or, how to turn a bog turtle into a spotted turtle to analyze both. Evolution. 63:1348–1355.
Strait D.S., Wang Q., Dechow P.C., Ross C.F., Richmond B.G., Spencer M.A., Patel B.A. 2005. Modeling elastic properties in finite element analysis: how much precision is needed to produce an accurate model? Anat. Rec. 283A:275–287.
Therrien F. 2005a. Mandibular force profiles of extant carnivorans and implications for the feeding behaviour of extinct predators. J. Zool. London. 267:249–270.
Therrien F. 2005b. Feeding behaviour and bite force of sabretoothed predators. Zool. J. Linn. Soc. 145:393–426.
Timoshenko, S. P., 1922, On the transverse vibrations of bars of uniform cross-section, Phil. Mag. p. 125.
Thomason, J.J. 1991. Cranial strength in relation to estimated biting forces in some mammals. Can. J. Zool., 69: 2326-2333.
Tseng Z.J., Binder W.J. 2009. Mandibular biomechanics of *Crocuta crocuta*, *Canis lupus*, and the late Miocene *Dinocrocuta gigantea* (Carnivora, Mammalia). Zool. J. Linn. Soc. 158(3):683–696.
Tseng Z.J., Takeuchi G.T., Wang X. 2010. Discovery of the upper dentition of *Barbourofelis whitfordi* (Nimravidae, Carnivora) and an evaluation of the genus in California. J. Vert. Pal. 30(1):244–254.
Turner A., Antón M. 1997. The big cats and their fossil relatives. Columbia University Press, New York.
Van Valkenburgh B. 2007. *Déjà vu*: the evolution of feeding morphologies in the Carnivora. Integr. Comp. Biol. 47:147–163.
Van Valkenburgh B., Wayne, R.K. 2010. Carnivores. Curr. Biol. 20:R915–R919.
Warren J.C. 1853. Remarks on *Felis smylodon*. Proc. Boston Soc. Nat. Hist. 4:256–258.
Werdelin L., Lewis M.E. 2001. A revision of the genus *Dinofelis* (Mammalia, Felidae). Zool. J. Linn. Soc. 132:147–258.
Werdelin L., Peigné S. 2010. Carnivora. In: Werdelin L., Sanders W.J., editors. Cenozoic mammals of Africa. University of California Press. p. 603–657.
Werdelin L., Yamaguchi N., Johnson W.E., O'Brien S. J. 2010. Phylogeny and evolution of cats. In: MacDonald D.W., Loveridge A.J., editors. Biology and conservation of wild felids. New York: Oxford University Press. p. 59–82.
Wroe S., McHenry C., Thomason J.J. 2005. Bite club: comparative bite force in big biting mammals and the prediction of predatory behaviour in fossil taxa. Proc. R. Soc. Lond. B 272: 619–625.
Wroe S., Moreno K., Clausen P., McHenry C., Curnoe D. 2007. High-resolution three dimensional computer simulation of hominid cranial mechanics. Anat. Rec. 290:1248–1255.
Young R.L., Badyaev A.V.2006. Evolutionary persistence of phenotypic integration: Influence of developmental and functional relationships on evolution of complex trait. Evolution. 60:1291–1299.
Young M.T., Brusatte S.L., Ruta M., Andrade M.B. 2010. The evolution of Metriorhynchoidea (mesoeucrocodylia, thalattosuchia): an integrated approach using geometric morphometrics, analysis of disparity, and biomechanics. Zool. J. Linn. Soc. 158:801–859.
Zelditch M.L., Wood A.R., Swiderski, D.L. 2009. Building developmental integration into functional systems: function-induced integration of mandibular shape. Evol. Biol. New York. 36:71–87.
Zienkiewicz O.C., Taylor R.L., Zhu J.Z. 2005. The finite element method: its basis and fundamentals. IXth Edition. Elsevier.